

Unraveling Adaptive Evolutionary Divergence at Microgeographic Scales

Erin Clancey^{1,2,*} 0000-0003-4728-4023

Ailene MacPherson³ 0000-0003-1783-4127

Rebecca G. Cheek⁴ 0000-0002-7935-3153

James C. Mouton⁵ 0000-0002-8475-9078

T. Scott Sillett⁵ 0000-0002-7486-0076

Cameron K. Ghalambor^{4,6} 0000-0003-2515-4981

W. Chris Funk⁴ 0000-0002-6466-3618

Paul A. Hohenlohe^{1,7} 0000-0002-7616-0161

1. Department of Mathematics and Statistical Science, University of Idaho, Moscow, ID 83844 USA;
2. Current Address: Paul G. Allen School for Global Health, Washington State University, Pullman, WA 99164 USA;
3. Department of Mathematics, Simon Fraser University, Burnaby, BC, V5A 1S6, Canada;
4. Graduate Degree Program in Ecology, Department of Biology, Colorado State University, Fort Collins, Colorado 80523 USA;
5. Migratory Bird Center, Smithsonian's National Zoo and Conservation Biology Institute, Washington, DC 20013;
6. Department of Biology, Centre for Biodiversity Dynamics (CBD), Norwegian University of Science and Technology (NTNU), N-7491 Trondheim, Norway;
7. Department of Biological Sciences, Institute for Bioinformatics and Evolutionary Studies,

University of Idaho, Moscow, ID 83844 USA;

* Corresponding author; e-mail: erin.clancey@wsu.edu

Short Title: Divergence at Microgeographic Scales

Manuscript elements: Figure 1-5, Table 1-2, Appendix and Supplementary Material: Figure B1-B3, Zenodo Repository.

Keywords: phenotype-dependent dispersal, *Aphelocoma*, individual-based simulations, microgeographic evolutionary divergence, local adaptation, quantitative genetics models.

Manuscript type: E-article.

Prepared using the suggested L^AT_EX template for *Am. Nat.*

Abstract

Striking examples of local adaptation at fine geographic scales are increasingly being documented in natural populations. However, the relative contributions made by natural selection, phenotype-dependent dispersal (when individuals disperse with respect to a habitat preference), and mate preference in generating and maintaining microgeographic adaptation and divergence are not well studied. Here, we develop quantitative genetics models and individual-based simulations (IBS) to uncover the evolutionary forces that possibly drive microgeographic divergence. We also perform Bayesian estimation of the parameters in our IBS using empirical data on habitat-specific variation in bill morphology in the island scrub-jay (*Aphelocoma insularis*) to apply our models to a natural system. We find that natural selection and phenotype-dependent dispersal can generate the patterns of divergence we observe in the island scrub-jay. However, mate preference for a mate with similar bill morphology, even though observed in the species, does not play a significant role in driving divergence. Our modeling approach provides insights into phenotypic evolution occurring over small spatial scales relative to dispersal ranges, suggesting that adaptive divergence at microgeographic scales may be common across a wider range of taxa than previously thought. Our quantitative genetic models help to inform future theoretical and empirical work to determine how selection, habitat preference, and mate preference contribute to local adaptation and microgeographic divergence.

Introduction

Adaptive evolutionary divergence between populations has long been recognized to be governed by the balance between selection and gene flow. Environmental variation can impose divergent selection on populations resulting in local adaptation, but high gene flow can overwhelm local selection and prevent adaptive divergence (Blanquart et al., 2012; Kawecki and Ebert, 2004; Savolainen et al., 2013). The homogenizing effects of gene flow are expected to be especially important in limiting local adaptation across small geographic scales because dispersal is more likely across short distances. However, several recent empirical studies in a variety of taxa have demonstrated that divergence can occur within a population as a result of variation in biotic and abiotic conditions at small spatial scales (Bolnick et al., 2009; Garroway et al., 2013; Hays et al., 2021; Hendrick et al., 2016; Keller et al., 2013; Mikles et al., 2020; Richardson et al., 2014). The ecological and evolutionary mechanisms that promote microgeographic adaptation and divergence, processes that occur when dispersal is frequent enough to prevent divergence by genetic drift (Richardson et al., 2014), are critical for advancing our understanding of adaptation and diversity within populations. However, the spatial scale at which these mechanisms operate is poorly understood in natural systems (Richardson et al., 2014), and mechanisms generating divergence with gene flow other than natural selection remain underexplored.

When ecological optima vary between patches at small geographic scales, local adaptation is often attributed to strong natural selection (Bolnick and Otto, 2013). Selection of any strength will bring the population trait means closer to the local ecological optimum, but only strong selection can overcome high levels of migration occurring within a dispersal neighborhood (Tigano and Friesen, 2016) – the distance over which individuals regularly move within a generation (Wright, 1946). While natural selection is essential for local adaptation, other evolutionary forces such as nonrandom dispersal and local assortative mating may also play a significant role, particularly in the face of rapid migration (Berner and Thibert-Plante, 2015; Bolnick and Otto, 2013; Edelaar and Bolnick, 2012; Ravigné et al., 2009, 2004; Richardson et al., 2014). Phenotype-dependent

dispersal, in which dispersing individuals choose a habitat type according to how well their phenotype matches the ecological optima, is one such mode of non-random dispersal that can facilitate local adaptation, population divergence, and even reproductive isolation, as shown by both theoretical and empirical studies (Bolnick and Otto, 2013; Bolnick et al., 2009; Camacho et al., 2020; Edelaar and Bolnick, 2012; Levene, 1953; Maynard-Smith, 1966; Nicolaus and Edelaar, 2018; Ravigné et al., 2009). For example, in a theoretical study, Bolnick and Otto (2013) demonstrate that genotype-dependent dispersal can be responsible for the majority of divergence between neighboring populations, especially when dispersal rates are high, as would be the case at microgeographic scales. Similarly, Edelaar et al. (2019) show empirically that when individuals selectively move to improve the match between their trait values and the environmental characteristics, these matching habitat preferences can be an important driver of local adaptation. Once primary forces like strong natural selection or phenotype-dependent dispersal have created a bimodal trait distribution in a population, we understand from theoretical studies that local assortative mating arising from mate preferences can amplify divergence (Kirkpatrick and Nuismer, 2004; Kopp et al., 2018; Richardson et al., 2014; Servedio et al., 2011) and further enhance local or microgeographic adaptation. However, we have less knowledge about how all of these processes interact, especially in specific examples of natural systems.

A striking case of microgeographic divergence is observed in bill morphology in the island scrub-jay (*Aphelocoma insularis*), the only insular endemic landbird species in North America (Morrison et al., 2011). The entire island scrub-jay species range is just 250 km² on Santa Cruz Island off the coast of southern California, USA (Delaney and Cheek, 2022; Langin et al., 2015). Suitable island scrub-jay habitat covering Santa Cruz Island consists primarily of island scrub-oak (*Quercus pacifica*), and three geographically discrete woodland areas of bishop pine (*Pinus muricata*) stands. Island scrub-jay bill morphology, a primary determinant of foraging ability, is divergent between subpopulations residing in the oak and pine neighboring habitat types (Langin et al., 2015). A similar pattern is observed in the closely related California scrub-jay (*Aphelocoma californica*), whose morphological differences result in divergent feeding performance

on acorns versus pine cones (Bardwell et al., 2001; Peterson, 1993). Additionally, island scrub-jays mate non-randomly with respect to bill morphology, which may be due to variation in acoustic signal structure of female rattle calls caused by bill shape (Langin et al., 2015, 2017). Similar effects on vocal signals by selection on bill morphology have been suggested to occur in other bird species, and may drive reproductive isolation if the song is used in mate choice (e.g., Ballentine et al., 2013; Derryberry et al., 2012; Podos, 2001). It is therefore plausible that individual island scrub-jays would be under selection to exhibit a preference for habitats where their own trait value is closer to an ecological optimum, and also select mates based on an acoustic signal related to foraging ability. There is no evidence of gene flow from mainland species to confound patterns of divergence (Delaney and Wayne, 2005; DeRaad et al., 2022), and the repeated pine-oak transitions at fine spatial scales occur without any barriers to dispersal, allowing for high rates of movement between habitats (Cheek et al., 2022; Langin et al., 2015). The island scrub jay, therefore, represents a unique opportunity to study the evolutionary processes that contribute to microgeographic adaptation. We use the patterns of divergence in bill morphology, specifically bill length as our focal trait, between the pine and oak habitats in the island scrub-jay system to guide the development of our evolutionary models and test hypotheses about mechanisms capable of promoting and maintaining microgeographic divergence in wild populations.

To test alternative hypotheses about the specific mechanisms underlying microgeographic divergence in nature, we use analytical and individual-based simulation (IBS) models to understand divergence in a single phenotypic trait. First, we develop a general model using a theoretical quantitative genetics framework, because bill length is a quantitative trait with a polygenic basis (Cheek et al., 2022; Langin et al., 2015). We then analyze the model using strict, but necessary analytical approximations to uncover the dominant drivers of microgeographic divergence when dispersal occurs either randomly or dependent on phenotype, and in general to study phenotype-dependent dispersal mathematically. Next, while relaxing key assumptions, we use an IBS model parameterized with data from the island scrub-jay system to explore the evolutionary conditions that may have produced the observed patterns of divergence in bill morphology.

We also estimate the unknown parameter values in our IBS model by adapting the Metropolis-Hastings algorithm (Metropolis et al., 1953), a Bayesian Markov Chain Monte Carlo (MCMC) method, to accommodate our simulation-based likelihood approach. With the posterior distributions generated from our Bayesian estimation procedure, we address two questions motivated by observations of microgeographic evolution in the island scrub-jay system: (1) What are the primary drivers of the observed pattern of microgeographic divergence in the island scrub-jay: strong natural selection, phenotype-dependent dispersal, or a combination of the two forces? (2) Does mate preference for a mate with similar bill morphology amplify the observed divergence in the island scrub-jay?

The Empirical System

Study Site and Population

The island scrub-jay is a passerine bird endemic to Santa Cruz Island approximately 32 kilometers off the coast of southern California. Genomic data suggests the island scrub-jay has been evolving in isolation from its sister species (*A. californica*) for up to approximately one million years (DeRaad et al., 2022). On Santa Cruz Island, island scrub-jays forage and breed in both oak chaparral and pine woodland habitats. Divergence in bill morphology has been observed between island scrub-jays residing in each habitat. Individuals that occur in pine habitat have longer, shallower bills compared to individuals in adjacent oak habitat, which is likely due to differences in foraging ecology (Langin et al., 2015). Variation in bill morphology across habitats, however, cannot be explained by differential wear and tear. Seasonal variation in bill length does occur, but it is consistent across habitats (Langin et al., 2015), and bill morphology is a heritable trait (Cheek et al., 2022; Langin et al., 2015), suggesting these patterns are not simply due to plasticity. Sexual size dimorphism is also present in this population, where males are larger than females and have larger bills. Male-male competition for territories favors larger males and is likely responsible for body size and bill size differences between the sexes (Desrosiers et al.,

2021).

Morphological Data Collection

As part of a long-term study monitoring island scrub-jays on Santa Cruz Island (Caldwell et al., 2013; Cheek et al., 2022; Langin et al., 2015), the trait of interest, bill length, was measured in adult island scrub-jays that were captured with baited drop traps or mist nets from 2007–2020. Each individual was marked with a unique combination of numbered aluminum and colored leg bands and age was estimated according to plumage differences described by Pyle (1997). An individual’s bill length was measured from the anterior end of the nares to the tip of the bill using Mitutoyo digital calipers that have a resolution of 0.01 mm. Captured island scrub-jays were assigned to the pine or oak habitats based on the methods described in Cheek et al. (2022), which estimated the percent pine and percent oak within a 300-m radius of each scrub-jay sampling location (the diameter of the largest island scrub-jay territory; (Caldwell et al., 2013)) using a reclassified 2005 vegetation map of Santa Cruz Island (Langin et al., 2015; Nature Conservancy, 2007).

Population Estimates and Sample Statistics

According to vegetation surveys conducted by the Nature Conservancy (2007), about 88% of the island was classified as oak habitat and 12% was classified as pine habitat. Bakker et al. (2020) estimated the total island scrub-jay population size to be 1,803 individuals, and the habitat capacity for breeding pairs was estimated to be 515 territories across the entire island. We approximated the oak and pine subpopulation sizes and number of breeding territories in each habitat by combining the information from Bakker et al. (2020) and the proportion of habitat classification from the Nature Conservancy (2007), such that oak subpopulation size was 1587 with 453 breeding territories and the pine subpopulation size was 216 with 62 breeding territories. Caldwell et al. (2013) estimated the mean annual fecundity for breeding adult island scrub-jays

to be 1.1 ± 0.1 young fledged per breeding pair.

Using the measurements of bill length, we calculated sample statistics for each subpopulation by pooling observations of adult birds across all years of the study. For any individual with multiple measurements of bill length, we calculated the average measurement, as bill length changes little over an individual's adult lifetime. The difference in male bill length means between the oak and pine subpopulations was 0.79 mm, $p < 0.001$, calculated from a sample of 211 male oak birds and 92 male pine birds. The difference in female bill length means between the oak and pine subpopulations was 0.80 mm, $p < 0.001$, calculated from a sample of 175 female oak birds and 79 female pine birds. However, there was no significant difference in the variance of bill lengths (mm^2) between males and females in each habitat nor across habitats, so we calculated the composite phenotypic variance of the population, which was 1.30 mm^2 with 95% confidence interval (CI) [1.16, 1.47]. The mean difference in bill length (mm) between males and females across both subpopulations was 2.07 mm (we round to 2 mm for the simulations), $p < 0.001$. The trait distributions for males and females in the oak and pine habitats are shown in Figure 1.

In our model, local assortative mating within habitats and sexual selection is generated by a preference for mates with similar bill morphology. We used the maximum-likelihood approach from Clancey et al. (2022) that accommodates multiple discrete populations to estimate the strength of mate preference, α , and the preferred distance between male and female bill lengths, the match offset parameter δ (see Figure 2 Equation (2)), with data on 153 mated pairs of island scrub-jays. The strength of mate preference, α , dictates the width of the Gaussian function describing the probability of mating between a male and a female if they meet, and is equivalent to the inverse of two times the tolerance of this function from Lande (1981) (see Kirkpatrick and Nuismer, 2004). The match offset, δ , specifies the location of the center of this function. We estimated the strength of mate preference to be $\alpha = 0.1 \pm 0.073 \text{ mm}^{-2}$ (95% CI) and the optimal distance between male and female bill lengths within mated pairs, the match offset, to be $\delta = 2.0 \pm 0.80 \text{ mm}$ (95% CI). Both α and δ are significantly different from zero indicating that the population does not mate randomly according to bill length (e.g., $\alpha = 0$ indicates

a randomly mating population), and mate preferences contribute to the maintenance of sexual dimorphism.

Lastly, to estimate the random dispersal rate, m , between habitats on Santa Cruz Island, we calculated the fixation index (F_{st}) by comparing 88 individuals sampled in the oak habitat and 35 individuals sampled in the pine habitat genotyped at 3,408 neutral loci identified by Cheek et al. (2022). We then calculated the per generation dispersal rate by re-arranging the equation for F from Wright (1949) with an effective population size of 350 (Cheek et al., 2022) to get an estimate of $m = 0.084$. This estimate was used to generate the prior distribution for m in our Bayesian estimation procedure described below.

The General Model

To study microgeographic evolution in general and then specifically in the island scrub-jay system, we model a metapopulation consisting of an effectively infinite number of patches with two distinct habitat types, i , resembling the pine (P) and oak (O) habitat matrix on Santa Cruz Island (for example, $i = \{O, P\}$). The population is assumed to have been colonized by one founding population that then diverged *in situ*, and is now observed at the present day in eco-evolutionary equilibrium. Dispersal rates (m) between habitats are high ($N_i m \gg 1$ migrant per generation) and there are no physical barriers to movement. Individuals exhibit a single phenotypic trait, z , that is assumed to be controlled by a very large number of freely recombining additive loci of small effect, and a sex-specific effect generating sexual dimorphism, $\tilde{\delta}$, that causes male and female trait values to differ by a fixed amount. There are two ecological optima, one optimum in each habitat (e.g., θ_O and θ_P), and these ecological optima are the same for both sexes. Modeling a dioecious population, the trait value (z) of the k^{th} male or female is given by:

$$z_k = g_k + \epsilon_e + \begin{cases} +\tilde{\delta} & \text{male} \\ -\tilde{\delta} & \text{female} \end{cases}, \text{ where } g_k = g_{mid,k} + \epsilon_s. \quad (1)$$

Here g_k is the breeding value of individual k , which is assumed to be the mean of the breeding values of the parents ($g_{mid,k}$) of individual k , plus deviation ϵ_s due to segregational variance. The phenotypic trait value for each individual z_k , is the sum of the breeding value for individual k plus deviation ϵ_e due to environmental variance. The deviates ϵ_s and ϵ_e are drawn for each individual from two independent normal distributions with mean 0 and constant variances resulting from allelic segregation (σ_s^2) and random environmental factors (σ_e^2), respectively. In our model, the segregational variance (i.e., reflecting the genetic variance among full sibs) is roughly half the additive genetic variance at equilibrium and similar to the expectations given by Barton et al. (2017). The trait distributions in each subpopulation are also assumed to be normal, each with their own male and female means and variances, $Z_{M_i} \sim \mathcal{N}(\bar{z}_{M_i}, \mathcal{V}_{M_i})$ and $Z_{F_i} \sim \mathcal{N}(\bar{z}_{F_i}, \mathcal{V}_{F_i})$.

Our model follows individuals over a four-stage life cycle in which they undergo density-dependent population growth, mate and reproduce, disperse with the opportunity for habitat preference, and undergo selection within each habitat (Figure 2). Generations overlap, but there is no age structure. Offspring are formed and enter the population as adults, and reproduction and death occur independent of age. We assume population size is controlled through density-dependent survival such that the population cannot exceed the carrying capacities in each habitat defined in Figure 2 Equation (1). N is the total population size at carrying capacity, H_i is the proportional size of each habitat, i , and N_i is the carrying capacity in habitat i . The number of successfully mated pairs is limited to the number of nesting sites, n such that $nH_i \leq NH_i$, in each habitat.

After census, the life cycle continues to mating and reproduction (Figure 2). The probability of mating between two individuals is given by Figure 2 Equation (2), which depends on the distance between the male and female phenotypic trait values, the match offset value, δ , and the strength of mate preference, α (see Clancey et al., 2022). If the strength of mate preference, α , is zero, individuals mate randomly. If the strength of mate preference is non-zero, individuals prefer a similar mate relative to their own trait value, but with an optimal fixed difference between the male and female trait values given by the match offset, δ (Clancey et al., 2022). When a mated

pair forms successfully, reproduction is assumed to ensue and the mated pair raises one offspring that survives to adulthood (e.g., island scrub-jays on average raise one offspring that survives to leave the nest; see above).

After reproduction occurs, individuals are allowed to disperse from habitat j to habitat i according to the probability in Figure 2 Equation (3). The rate at which individuals leave their natal habitat patch and move to a new location, either switching habitat types or simply moving to a new location of the same habitat type, is given by the parameter m , the rate of random dispersal. The probability that an individual arrives in a particular habitat is proportional to the percentage of the landscape covered by that habitat, H_i where $\sum_i H_i = 1$. Since the probability of arrival depends on the spatial size of each habitat and the subpopulation sizes are defined by the habitat sizes (Figure 2 Equations (1) and (3)), this results in an equal number of migrants exchanged across habitats in each generation. If individuals display a habitat preference (i.e., when the parameter η is non-zero) individuals will move non-randomly according to the distance between their trait value and the ecological optimum in each habitat (θ_i). When $\eta = 0$, dispersal occurs randomly with probability mH_i . In the case of equal habitat sizes, Figure 2 Equation (3) is the quantitative trait analog to the genetic model of habitat selection as given by Equation 4 in Bolnick and Otto (2013). Figure 3 shows the probability of dispersal in Figure 2 Equation (3) when the habitat sizes are the same ($H_i = H_j$ and j is an alternative habitat to i) and when the habitat sizes are asymmetric ($H_i \neq H_j$) for different values of the parameter η .

Once individuals disperse, they must undergo viability selection in each environment. The probability of survival decays in a Gaussian fashion according to Figure 2 Equation (4) as a function of the strength of natural selection, γ , and the difference between an individual's trait value and the ecological optimum in the habitat of residence, θ_i . This four-stage life cycle forms the basis for our analytical approximations and individual-based simulation (IBS) models.

Analytical Approximations

We begin by analyzing the general model with analytical approximations, which are necessarily strict for tractability, to identify potential drivers and conditions required for microgeographic divergence in phenotypic trait means at evolutionary equilibrium ($\delta_{\bar{z}_{eq}}$). Specifically, our analytical approximations make the following explicit assumptions to model divergence between habitats in a two-patch model: (i) The distance between each individual's trait value and the ecological optimum in the habitat of residence is small such that $z - \theta_i = \mathcal{O}(\epsilon)$, (ii) the distance between the ecological optima is small such that $\theta_j - \theta_i = \delta_\theta = \mathcal{O}(\epsilon)$, (iii) additive genetic variance, G , is constant and equal across subpopulations, (iv) random mating ($\alpha = 0$) occurs within each subpopulation, and (v) there is no sexual dimorphism ($\tilde{\delta} = 0$). Assumption (i) ensures that the effects of both selection (γ) and habitat preference (η) are weak and assumption (ii) ensures that selection is weak on migrants in both habitats. The combination of assumptions (i)-(iii) has the restrictive consequence that additive genetic variation is not only constant but very small and is of $\mathcal{O}(\epsilon^2)$. These five assumptions, along with the assumption that phenotypes are normally distributed, allow us to use standard quantitative genetics approaches similar to Falconer and Mackay (1996) to obtain tractable analytical results. Analytical approximations were performed using Wolfram Mathematica 12.3 (Wolfram Research, Inc., 2021).

We follow the equations that model the life cycle under the assumptions outlined above to solve a series of recursions to find the equilibrium phenotypic divergence between habitats ($\delta_{\bar{z}_{eq}}$). At census, the subpopulations each have their own unique trait means, \bar{z}_i . Given the assumption of random mating, the mean phenotype of each subpopulation remains unchanged by reproduction such that $\bar{z}'_i = \bar{z}_i$, and $f'_i(z)$ is the distribution of the trait in habitat i after reproduction. We can now use the distribution $f'_i(z)$ and the dispersal function in Figure 2 Equation (3) to describe the subpopulation means after phenotype-dependent dispersal as:

$$\bar{z}_i'' = \int_{-\infty}^{\infty} z f_i''(z) dz = \frac{\int_{-\infty}^{\infty} z \left(f_i'(z) H_i (1 - \mathcal{P}(i \rightarrow j|z)) + f_j'(z) H_j \mathcal{P}(j \rightarrow i|z) \right) dz}{\int_{-\infty}^{\infty} f_i'(z) H_i (1 - \mathcal{P}(i \rightarrow j|z)) + f_j'(z) H_j \mathcal{P}(j \rightarrow i|z) dz}. \quad (2)$$

Following phenotype-dependent dispersal, the change in the mean phenotype in habitat i due to selection proceeds as given by Equation 7 in Lande (1976):

$$\Delta \bar{z}_i''' = G \frac{d \bar{W}}{d \bar{z}_i''} = G \frac{d}{d \bar{z}_i''} \mathbb{E} \left[e^{-\gamma(z - \theta_i)^2} \right], \quad (3)$$

and allows us to calculate the phenotypic mean after phenotype-dependent dispersal and selection as $\bar{z}_i''' = \bar{z}_i'' + \Delta \bar{z}_i'''$ in each habitat.

Assuming that the distance between the ecological optima, δ_θ , and the distance $z_i - \theta_i$ are both small and of $\mathcal{O}(\epsilon)$, we can approximate these distances to $\mathcal{O}(\epsilon^2)$ to obtain the Taylor series approximations for Equations (2) and (3) giving us an approximation for the subpopulation means in each habitat after reproduction, dispersal, and selection, \bar{z}_i''' and \bar{z}_j''' (see Appendix A). Solving these recursions, we have the analytical approximation for phenotypic divergence at evolutionary equilibrium, $\delta_{\bar{z}_{eq}} = \bar{z}_{eq_j} - \bar{z}_{eq_i}$:

$$\delta_{\bar{z}_{eq}} \approx \frac{-\delta_\theta 2G\gamma}{m(2G\gamma - 1) - 2G\gamma}. \quad (4)$$

Notably, Equation (4) does not contain η , habitat preference, once we make our assumptions and approximate the dynamical equations to $\mathcal{O}(\epsilon^2)$. The diversifying effect of phenotype-dependent dispersal is of $\mathcal{O}(\epsilon^3)$, and hence drops out of the approximation. This is because it depends on the product of the distance between the optima (δ_θ), which is $\mathcal{O}(\epsilon)$, and the phenotypic variance (\mathcal{V}_z), which is $\mathcal{O}(\epsilon^2)$ (see Appendix A). When the distance between the ecological optima is small and the distance between the subpopulation means and their corresponding ecological optimum value is also small, phenotype-dependent dispersal has a negligible biological effect, and the solution seen in Equation (4) reduces approximately to the balance between selection and gene flow. Therefore, phenotype-dependent dispersal that generates phenotypic

divergence requires either strong habitat preference (η), large environmental differences (δ_θ), or both, and modeling these conditions requires a simulation-based approach.

Individual-Based Simulations and Bayesian Parameter Estimation

To model microgeographic divergence with respect to the island scrub-jay system, we use individual-based simulations (IBS) to relax key assumptions present in the analytical approximations and introduce stochasticity. The IBS model follows individual male and female island scrub-jays throughout the life cycle of the general model using the equations presented in Figure 2 and the production of offspring according to Equation (1). The IBS model extends beyond the analytical model above in several ways: habitat preference (η) and natural selection (γ) can be strong, individuals mate with a preference for a mate whose trait value is δ away from their own, the sex ratio is equal but the sexes are dimorphic by a fixed amount given by $\tilde{\delta}$, and genetic variance, measured by the variance in breeding values, and phenotypic variances can now vary from one generation to the next (even though segregational variance, σ_s^2 , is constant).

The simulation model is initiated by drawing breeding values for males and females in the oak and pine subpopulations from a normal distribution with identical means equal to the ecological optimum for the oak habitat with a fixed value for additive genetic variance of $G = 1.0$. Trait values are assigned to each individual according to Equation (1), where g_k is the initial breeding value and the sexual-dimorphism parameter is $\tilde{\delta} = 1$. Individuals then choose mates, disperse, and survive as a function of their trait values using Equations (2), (3) and (4) in Figure 2. We assume a fixed number of breeding territories are available and scaled by the size of each habitat such that not all individuals in the population get the opportunity to reproduce (Table 1). If a successful pairing occurs, one offspring is produced according to Equation (1). These offspring enter the population as adults and disperse according to Figure 2 Equation (3). Next, individuals survive or die according to the probability calculated from Figure 2 Equation (4) (viability selection). Last, density-dependent regulation is applied to individuals randomly re-

gardless of their phenotype or age, so the total population size (N) remains at carrying capacity. The population mean breeding values and trait values are allowed to evolve for a maximum of 1,000 generations or until evolutionary equilibrium is reached. Figure B1 in the Supplemental shows an example of the subpopulation male and female means and variances at equilibrium after 1,000 generations. All variance terms in the IBS are given as standard deviations (see Table 1).

We use our IBS to estimate the parameters in our model with the data on bill length (mm) in the island scrub-jay. To implement our Bayesian estimation procedure using the Metropolis-Hastings algorithm (Metropolis et al., 1953), we simulate the life cycle to generate the joint distribution of phenotypes for males and females in each subpopulation, $f_{Z_{M_i}, Z_{F_i}, Z_{M_j}, Z_{F_j}}(z_{M_i}, z_{F_i}, z_{M_j}, z_{F_j}; \theta)$, where $\theta = (\eta, \theta_i, \theta_j, \gamma, \sigma_e, \sigma_s)'$, and N , H_O and H_P , α , δ , and $\tilde{\delta}$ are known and fixed (Table 1). Because we assume the infinitesimal model, we also assume that once evolutionary equilibrium is reached at any time point, t , measured in discrete generations, the marginal distribution of each subpopulation is normal such that $Z_{M_i,t} \sim \mathcal{N}(\mu_{M_i,t}|\theta, \sigma_{M_i,t}^2|\theta)$, $Z_{F_i,t} \sim \mathcal{N}(\mu_{F_i,t}|\theta, \sigma_{F_i,t}^2|\theta)$, $Z_{M_j,t} \sim \mathcal{N}(\mu_{M_j,t}|\theta, \sigma_{M_j,t}^2|\theta)$, and $Z_{F_j,t} \sim \mathcal{N}(\mu_{F_j,t}|\theta, \sigma_{F_j,t}^2|\theta)$. We also assume that the observations $z_{k,M_i,t}^*$, $z_{k,M_j,t}^*$, $z_{k,F_i,t}^*$ and $z_{k,F_j,t}^*$ were sampled independently allowing us to formulate the likelihood function by multiplying these four distributions:

$$\mathcal{L}(\theta) = \prod_{k \in M_i} \frac{\exp\left[-\frac{1}{2}\left(\frac{z_{k,M_i,t}^* - \mu_{M_i,t}|\theta}{\sigma_{M_i,t}|\theta}\right)^2\right]}{\sigma_{M_i,t}|\theta\sqrt{2\pi}} \times \prod_{k \in F_i} \frac{\exp\left[-\frac{1}{2}\left(\frac{z_{k,F_i,t}^* - \mu_{F_i,t}|\theta}{\sigma_{F_i,t}|\theta}\right)^2\right]}{\sigma_{F_i,t}|\theta\sqrt{2\pi}} \\ \times \prod_{k \in M_j} \frac{\exp\left[-\frac{1}{2}\left(\frac{z_{k,M_j,t}^* - \mu_{M_j,t}|\theta}{\sigma_{M_j,t}|\theta}\right)^2\right]}{\sigma_{M_j,t}|\theta\sqrt{2\pi}} \times \prod_{k \in F_j} \frac{\exp\left[-\frac{1}{2}\left(\frac{z_{k,F_j,t}^* - \mu_{F_j,t}|\theta}{\sigma_{F_j,t}|\theta}\right)^2\right]}{\sigma_{F_j,t}|\theta\sqrt{2\pi}}. \quad (5)$$

Using this formulation of the likelihood function, we implement the Metropolis-Hastings algorithm to sample from the joint posterior distribution of our model parameters and estimate the unknown values (see Supplemental for additional information on our Bayesian parameter estimation procedure). A list of parameter symbols and values used in the IBS model is shown

in Table 1. Prior distributions of the unknown parameters are uniform and cover a biologically plausible range, and the dispersal parameter, m , is drawn from a gamma distribution with a mode of 0.084, because m cannot be less than zero and F_{st} provides a rough estimate of m . The IBS and Bayesian estimation procedure was developed in R (R Core Team, 2021).

Table 1: Parameters governing the Individual-Based Simulations (IBS). The estimation column describes if parameter values were directly estimated with data from another study or from the empirical data collected in this study, or estimated from the IBS in this study. The method column describes if the parameter value is fixed across all simulations or is drawn from a prior distribution during the Bayesian Parameter Estimation. Fixed values and prior distributions are specified in the column labeled Value/Prior.

Parameter	Estimation	Method	Value/Prior	Description
N	Direct	Fixed	1803	Total population size at carrying capacity
n	Direct	Fixed	515	Total number of nesting sites
H_O, H_P	Data	Fixed	0.88, 0.12	Proportion habitat coverage
$\tilde{\delta}$	Data	Fixed	1 mm	Deviate generating sexual dimorphism
α	Direct	Fixed	0.1 mm^{-2}	Mate preference
δ	Direct	Fixed	2.0 mm	Mate preference offset match
γ	IBS	Random	$\mathcal{U}(0, 0.3) \text{ mm}$	Natural selection
η	IBS	Random	$\mathcal{U}(0, 0.3) \text{ mm}$	Habitat preference
θ_O	IBS	Random	$\mathcal{U}(20, 30) \text{ mm}$	Ecological optimum in Oak
θ_P	IBS	Random	$\mathcal{U}(20, 30) \text{ mm}$	Ecological optimum in Pine
σ_e	IBS	Random	$\mathcal{U}(0.5, 1.5) \text{ mm}$	Environmental standard deviation
σ_s	IBS	Random	$\mathcal{U}(0.5, 1.5) \text{ mm}$	Segregational standard deviation
m	IBS	Random	$\Gamma(9.4, 0.01)$	Probability of dispersal

Primary Mechanism of Microgeographic Divergence

To answer our first question about the primary evolutionary mechanism driving microgeographic divergence in the island scrub-jay, we interpret the parameter estimates obtained from

the joint posterior distribution from our Bayesian estimation procedure. We use the modes of the univariate posterior distributions as point estimates for each parameter, and compute the 95% highest density interval (HDI) to assess the uncertainty around these point estimates (Table 2; Figure B2). The point estimates and 95% HDIs for natural selection (γ) and habitat preference (η) are 0.0057 and [0, 0.02], and 0.21 and [0.05, 0.3], respectively. The point and interval estimates for γ demonstrate that natural selection can be weak when it operates locally in each habitat. For example, the probability of survival for a bird whose phenotype matches the opposite ecological optimum of their current habitat of residence is reduced by 1.3% using the point estimates in Table 2. The 95% HDI for γ includes zero, meaning that natural selection is not always required for divergence in the island scrub-jay, and does not include higher values of γ showing again that selection is weak. Conversely, the 95% HDI for habitat preference (η) does not include zero, and we find that divergence is not possible if habitat preference is too weak. The interval estimate for η also supports the results from our analytical approximations, that small values of η have little effect on divergence. Using the estimated values of m and η in Table 2, the proportion of oak habitat (88%) and pine habitat (12%) covering the island, and empirical population means from Figure 1, we calculate the probability an individual switches habitats, $\mathcal{P}(j \rightarrow i|z)$, following Figure 2 Equation (3). The probability an average female oak bird moves to the pine habitat is 3.3×10^{-7} , the probability an average male oak bird moves to the pine habitat is 0.018, the probability an average female pine bird moves to the oak habitat is 0.15, and the probability that an average male pine bird moves to the oak habitat is 0.00013. The probability of switching habitats depends on all of the parameters mentioned above and on an individual's bill length, and results in sex-specific migration.

Table 2: Parameter estimates given by the marginal posterior modes and the 95% Highest Density Interval (HDI).

Parameter	Definition	Estimate	95% HDI
η	Habitat preference	0.21	[0.05,0.30]
γ	Natural selection	0.0057	[0,0.02]
θ_O	Ecological optimum in Oak	23.68	[23.08,24.08]
θ_P	Ecological optimum in Pine	25.21	[24.23,26.78]
σ_e	Environmental standard deviation	0.83	[0.5,1.09]
σ_s	Segregational standard deviation	0.60	[0.5,0.89]
m	Probability of dispersal	0.084	[0.08,0.09]

Figure 4 shows the bivariate posterior distributions of η and γ in panel A, η and the distance between the ecological optima ($\delta_\theta = \theta_P - \theta_O$) in panel B, and γ and δ_θ in panel C. Figure 4 offers a two-dimensional view of the likelihood surface so that we can observe ridges caused by interactions between parameters and see which parameter combinations have the highest densities. Here we can again observe the broad range of the posterior distribution of η , and the ridges in the likelihood surface that correspond to all the values of η that maximize the likelihood for the data. All parameters shown in Figure 4 are negatively correlated with one another. The correlation between η and δ_θ is -0.38. When the ecological optima are closer together stronger habitat preference is required to reach the same degree of phenotypic divergence. The correlation between γ and η is -0.14. As habitat preference decreases, stronger selection is required for divergence to occur. The correlation between γ and δ_θ is -0.34. As δ_θ decreases, stronger selection is again required for divergence to occur. The interactions between parameters demonstrate that the distance between the ecological optima is also important to how we understand divergence generated by phenotype-dependent dispersal. Thus, with the estimated probability of random dispersal, $m = 0.084$ (Table 2), phenotype-dependent dispersal is required to generate divergence, while natural selection is likely weak, but not required to generate the divergence observed in bill

length, and the distance between the ecological optima is important in determining the dynamics of the evolutionary trajectory of the island scrub-jay across the oak and pine habitats.

Effect of Local Assortative Mating on Microgeographic Divergence

Island scrub-jays display a preference for a mate with similar bill morphology (Langin et al., 2015, 2017). We estimated the strength of mate preference ($\alpha = 0.1 \text{ mm}^{-2}$) in this study while accounting for population substructure, such that our value of α defines the strength of mate preference within each habitat, thus generating local assortative mating. To answer our second question addressing the conditions in which mate preference amplifies microgeographic divergence, we re-sample parameter combinations from the multivariate posterior distribution, set α equal to zero, and re-simulate the IBS to generate a null distribution of differences between trait values (δ_z) across habitats in males and females (Figure 5). We compare this distribution to the divergence we measure in the actual island scrub-jay population (Figure 5), and we find that mate preference for a mate with similar bill morphology does not amplify microgeographic divergence in this system.

Discussion

Even while arguing against the possibility of sympatric speciation, Ernst Mayr (1947) acknowledged that “all geographical barriers are relative,” and we can observe many cases of “microgeographical isolation” giving rise to new populations in nature even in the face of gene flow. In agreement with Mayr’s perspective, our results offer further evidence that microgeographic divergence in the complete absence of barriers to movement can be achieved under different evolutionary conditions. Here, we studied the effects of natural selection, phenotype-dependent dispersal, and mate preferences that generate local assortative mating in a two-patch model assuming the infinitesimal model of polygenic inheritance. We analyzed our general model in two ways: first, using mathematical analyses of quantitative genetics approximations

and second, with individual-based simulations (IBS). We find that the approximations required for a mathematical analysis of our model are so strict that it is difficult to gain general insights about phenotype-dependent dispersal. Specifically, when we make the assumptions that the distance between the ecological optima and the distance between an individual's trait value and the optimum of residence are both small (i.e. selection is weak within and between patches), the contribution of phenotype-dependent dispersal to divergence is negligible (i.e., of third order). However, this is not the case when the above assumptions are relaxed, and selection and habitat preference are moderate or strong. Thus, IBS are a more appropriate tool to study the effects of phenotype-dependent dispersal on divergence and allow us to apply our model to the island scrub-jay system.

The island scrub-jay is one example of a population exhibiting microgeographic evolutionary divergence, and we know there are preference for mates with a similar bill morphology in this population from both previous studies (Langin et al., 2015, 2017) and this study. The observations of divergence in bill morphology and mate preference in the island scrub-jay allow us to make a comparison between a natural system and our theoretical models to test hypotheses about the evolutionary mechanisms driving microgeographic divergence. Specifically, we applied our IBS model to the island scrub-jay to understand how natural selection, phenotype-dependent dispersal, and mate preference, contribute to divergence in bill morphology between the pine and oak habitats on Santa Cruz Island. To test our hypotheses, we estimated the parameters in our IBS model using a Bayesian framework by adapting the Metropolis-Hastings algorithm to accommodate the use of our IBS to evaluate a likelihood function. By obtaining estimates of the parameters in our IBS model, we found that strong natural selection is not required as a primary driver of divergence, phenotype-dependent dispersal is required to generate and maintain microgeographic divergence, and mate preference for a mate with similar bill morphology does not contribute to microgeographic divergence in this system.

Models of migration-selection balance are abundant, but the impact of habitat preference generating phenotype-dependent dispersal on evolutionary diversification has been insufficiently

modeled and explored (Berner and Thibert-Plante, 2015; Edelaar et al., 2008), especially in a microgeographic context. It is often assumed that strong selection is a requirement to overcome the homogenizing effects of gene flow when dispersal rates are high between populations (Haldane, 1930; Richardson et al., 2014). Our results demonstrate that this is not always the case; strong natural selection is not always a requirement if dispersal is phenotype-dependent. In agreement with other studies on non-random dispersal (e.g., Berner and Thibert-Plante, 2015; Bolnick and Otto, 2013; Bolnick et al., 2009; Camacho et al., 2020; Edelaar and Bolnick, 2012; Ravigné et al., 2009, 2004), we find that phenotype-dependent dispersal is a potent force of evolutionary divergence and can even drive divergence in the absence of selection. In support of this finding, Berner and Thibert-Plante (2015) show that habitat preferences can evolve during the process of adaptive divergence, and then facilitate divergence in the face of high dispersal propensities. We also find that in a heterogeneous environment with spatially varying ecological optima, the distance between the optima dictates how effective habitat preference can be at generating divergence. If individuals moving between habitats substantially fit better in a particular environment and have a preference to disperse to areas where they have higher fitness, the subpopulation phenotypes will diverge. But as the distance between ecological optima decreases, regardless of strong habitat preference, dispersal in the overall population will approach random movement and divergence will be minimal.

In many evolutionary scenarios, assortative mating generating sexual selection within localized patches can increase divergence by selecting against migrants and promoting local adaptation (Thibert-Plante and Hendry, 2009). However, the diversifying effects of local assortative mating are capricious. Assortative mating can sometimes (Kondrashov and Shpak, 1998), but not always generate evolutionary divergence (Kirkpatrick and Nuismer, 2004). As in many other studies, assortative mating in our model induces positive frequency-dependent sexual selection (because rare phenotypes have a higher chance of rejecting potential mates and thus losing of opportunities for reproduction). Previous studies have shown that sexual selection of this kind can be very effective in maintaining and amplifying divergence once it has been established

(Kirkpatrick and Nuismer, 2004; Richardson et al., 2014), but may impede divergence as long as the trait distribution is still bimodal (effectively acting as stabilizing selection; (Kirkpatrick and Nuismer, 2004; Kopp et al., 2018). Here, preference for a similar mate is the force generating local assortative mating within each habitat in our model, and mate preference is present in our empirical system. Yet, we find that the mate preference we observe in the island scrub-jay does not contribute to the divergence in bill morphology we observe. This could occur because the ecological optima are not far enough apart such that the phenotypic distribution of the overall population has not achieved enough bimodality for the observed mate preferences to have an amplifying effect on divergence in the bill length.

Although our analytical models and individual-based simulations offer general and informative results, they rely on limiting assumptions and ignore other key factors that we know can impact ecological and evolutionary dynamics. For example, we did not study phenotype-dependent dispersal when there is a cost associated with preferential migration (i.e., energetic costs of sampling habitat types or lost opportunity to find mates), nor did we study the effects of sex-specific habitat preference even though our population is sexually dimorphic. We assume the ecological optima for males and females are equivalent, but this might not be true in nature. In nature, individuals may pay the cost of being too choosy and this could alter the evolutionary dynamics we find in our results (Ravigné et al., 2009). Dispersers in nature must also balance finding breeding opportunities with foraging efficiency, and this dynamic is not included in our models and these effects could differ between the sexes. Our model also ignores intraspecific competition occurring between individuals within habitats for foraging areas and nesting sites. Individual scrub-jays vary in competitive ability, where larger individuals can secure territories and initiate breeding at younger ages (e.g., Desrosiers et al. 2021). Although we model asymmetric population sizes, we assume an exchange of migrants from the larger oak population to the smaller pine population occurs in equal numbers, and that settlement is not impacted by competitive ability. Alternatively, migrant exchange could be unequal, especially if migrants have different competitive abilities depending on their habitat of origin. Methodologically, our

Bayesian estimation procedure relies heavily on simulation-based methods to accomplish a high-dimensional optimization problem. Estimating many parameters from one dataset is challenging because high-dimensional posterior distributions often have a non-zero covariance structure (Gelman et al., 2013). Both the number of parameters and the correlations between them likely contribute to the uncertainty surrounding our point estimates. This could be alleviated in future studies if we were able to estimate some of these parameters independent from our IBS using another method. Finally, in our models we assume an infinitesimal model of genetic variation in a phenotypic trait. This model is limiting but also allows us to study phenotypic evolution in the absence of empirical knowledge of the exact number of loci that contribute to bill length variation in island scrub-jays. Thus, this model is rooted in quantitative genetics and intended to reflect the general case of a continuously varying, polygenic trait. Alternative models could test other scenarios, such as a few loci of large effect. As a point of comparison, Bolnick and Otto (2013) used a single-locus model and also found that phenotype-dependent dispersal can be an important factor in phenotypic divergence between habitats.

Even with these limitations, the results of our models have wide-ranging implications for the study of microgeographic evolution, both in theoretical and empirical studies. Conventional thinking has held that divergence and adaptation occurring at small spatial scales are rare evolutionary processes (Richardson et al., 2014). We have shown here that microgeographic divergence can easily be achieved if the appropriate conditions are present. Microgeographic divergence can occur with weak or no natural selection as long as phenotype-dependent dispersal is operating in a population. Since we have shown that microgeographic divergence can develop, many microgeographic evolutionary processes that are considered rare may be operating in more populations than expected. This conclusion leads to two implications. First, if microgeographic divergence and adaptation occur more commonly than previously detected in a wide range of taxa, these processes and their outcomes may be overlooked because they require careful observation and measurement to detect. Second, if microgeographic isolation is more common than previously thought, these evolutionary mechanisms promoting and maintaining divergence at small spatial

scales may be a cryptic force driving divergence events. If this is the case, we should more often consider microgeographic adaptation as an important process giving rise to incipient lineages. More empirical and theoretical research is needed to determine the circumstances under which microgeographic adaptation leads to reproductive isolation and speciation, and how the interplay between natural selection, phenotype-dependent dispersal, local assortative mating, and environmental conditions facilitate divergence.

Acknowledgments

We thank Scott L. Nuismer for the discussion of ideas and guidance in developing the analytical model and simulations, Luke J. Harmon for help developing the first version of the individual-based simulations, the many field technicians for their assistance with this project, Scott A. Morrison for his long-term support and collaboration on the Island Scrub-Jay Project, and the Editor Jennifer Lau, the Associate Editor Michael Kopp, and two Reviewers for helpful discussion and comments on the manuscript. Funding was provided by the U.S. National Science Foundation (DEB-1754821 and DEB-1754816 to WCF, CKG, TSS, and PAH), The Nature Conservancy (TNC), Colorado State University, and the Smithsonian Institution. We are grateful for the support provided by TNC staff, Channel Islands National Park, and the University of California Natural Reserve System's Santa Cruz Island Reserve. All work with living birds was approved by the Institutional Animal Care and Use Committees at Colorado State University (IACUC: #887) and the Smithsonian Institution.

Statement of Authorship

All co-authors contributed greatly to the conceptualization of this project over many successive discussions. The empirical data was collected by RGC, JCM, CKG, WCF, and TSS. The analytical model was designed by EC and AM and analyzed by AM. The individual-based simulations were designed by EC and PAH. EC developed and implemented the Bayesian estimation proce-

dure and performed the analyses to estimate parameters. EC wrote the manuscript, which was reviewed by all co-authors.

Data and Code Availability

The data, Mathematica Notebook, and R code supporting this publication are publicly available at <https://doi.org/10.5281/zenodo.8212987>.

Literature Cited

- Bakker, V. J., T. S. Sillett, W. M. Boyce, D. F. Doak, T. W. Vickers, W. K. Reisen, B. S. Cohen, M. T. Hallworth, and S. A. Morrison. 2020. Translocation with targeted vaccination is the most effective strategy to protect an island endemic bird threatened by West Nile virus. *Diversity and Distributions* 26:1104–1115.
- Ballentine, B., B. Horton, E. T. Brown, and R. Greenberg. 2013. Divergent selection on bill morphology contributes to nonrandom mating between swamp sparrow subspecies. *Animal Behaviour* 86:467–473.
- Bardwell, E., C. W. Benkman, and W. R. Gould. 2001. Adaptive geographic variation in western scrub-jays. *Ecology* 82:2617–2627.
- Barton, N. H., A. M. Etheridge, and A. Véber. 2017. The infinitesimal model: Definition, derivation, and implications. *Theoretical population biology* 118:50–73.
- Berner, D., and X. Thibert-Plante. 2015. How mechanisms of habitat preference evolve and promote divergence with gene flow. *Journal of evolutionary biology* 28:1641–1655.
- Blanquart, F., S. Gandon, and S. L. Nuismer. 2012. The effects of migration and drift on local adaptation to a heterogeneous environment. *Journal of evolutionary biology* 25:1351–1363.

- Bolnick, D. I., and S. P. Otto. 2013. The magnitude of local adaptation under genotype-dependent dispersal. *Ecology and Evolution* 3:4722–4735.
- Bolnick, D. I., L. K. Snowberg, C. Patenia, W. E. Stutz, T. Ingram, and O. L. Lau. 2009. Phenotype-Dependent Native Habitat Preference Facilitates Divergence Between Parapatric Lake and Stream Stickleback. *Evolution* 63:2004–2016.
- Caldwell, L., V. J. Bakker, T. Scott Sillett, M. A. Desrosiers, S. A. Morrison, and L. M. Angeloni. 2013. Reproductive ecology of the island scrub-jay. *The Condor* 115:603–613.
- Camacho, C., A. Sanabria-Fernández, A. Baños-Villalba, and P. Edelaar. 2020. Experimental evidence that matching habitat choice drives local adaptation in a wild population. *Proceedings of the Royal Society B* 287:20200721.
- Cheek, R. G., B. R. Forester, P. E. Salerno, D. R. Trumbo, K. M. Langin, N. Chen, T. Scott Sillett, S. A. Morrison, C. K. Ghalambor, and W. Chris Funk. 2022. Habitat-linked genetic variation supports microgeographic adaptive divergence in an island-endemic bird species. *Molecular Ecology* .
- Clancey, E., T. R. Johnson, L. J. Harmon, and P. A. Hohenlohe. 2022. Estimation of the strength of mate preference from mated pairs observed in the wild. *Evolution* 76:29–41.
- Delaney, K. S., and R. G. Cheek. 2022. Island scrub-jay (*aphelocoma insularis*), version 2.0. Birds of the World page <https://doi.org/10.2173/bow.issjay.02>.
- Delaney, K. S., and R. K. Wayne. 2005. Adaptive units for conservation: Population distinction and historic extinctions in the Island Scrub-Jay. *Conservation Biology* 19:523–533.
- DeRaad, D. A., J. E. McCormack, N. Chen, A. T. Peterson, and R. G. Moyle. 2022. Combining species delimitation, species trees, and tests for gene flow clarifies complex speciation in scrub-jays. *Systematic Biology* 71:1453–1470.

- Derryberry, E. P., N. Seddon, S. Claramunt, J. A. Tobias, A. Baker, A. Aleixo, and R. T. Brumfield. 2012. Correlated evolution of beak morphology and song in the neotropical woodcreeper radiation. *Evolution* 66:2784–2797.
- Desrosiers, M. A., K. M. Langin, W. C. Funk, T. S. Sillett, S. A. Morrison, C. K. Ghalambor, and L. M. Angeloni. 2021. Body size is associated with yearling breeding and extra-pair mating in the Island Scrub-Jay. *The Auk* 138:ukab045.
- Edelaar, P., A. Baños-Villalba, D. P. Quevedo, G. Escudero, D. I. Bolnick, and A. Jordán-Andrade. 2019. Biased movement drives local cryptic coloration on distinct urban pavements. *Proceedings of the Royal Society B* 286:20191343.
- Edelaar, P., and D. I. Bolnick. 2012. Non-random gene flow: an underappreciated force in evolution and ecology. *Trends in ecology & evolution* 27:659–665.
- Edelaar, P., A. M. Siepielski, and J. Clobert. 2008. Matching habitat choice causes directed gene flow: a neglected dimension in evolution and ecology. *Evolution: International Journal of Organic Evolution* 62:2462–2472.
- Falconer, D. S., and T. F. C. Mackay. 1996. *Introduction to Quantitative Genetics*. 4th ed. Pearson Education Limited, Essex, England.
- Garroway, C. J., R. Radersma, I. Sepil, A. W. Santure, I. De Cauwer, J. Slate, and B. C. Sheldon. 2013. Fine-scale genetic structure in a wild bird population: The role of limited dispersal and environmentally based selection as causal factors. *Evolution* 67:3488–3500.
- Gelman, A., J. B. Carlin, H. S. Stern, D. B. Dunson, A. Vehtari, and D. B. Rubin. 2013. *Bayesian data analysis Third Edition*. Chapman and Hall/CRC.
- Haldane, J. B. S. 1930. A mathematical theory of natural and artificial selection.(Part VI, Isolation.). Pages 220–230 *in* Mathematical proceedings of the Cambridge philosophical society. Vol. 26. Cambridge University Press.

- Hays, C., T. Hanley, A. Hughes, S. Truskey, R. Zerebecki, and E. Sotka. 2021. Local adaptation in marine foundation species at microgeographic scales. *The Biological Bulletin* 241:16–29.
- Hendrick, M. F., F. R. Finseth, M. E. Mathiasson, K. A. Palmer, E. M. Broder, P. Breigenzer, and L. Fishman. 2016. The genetics of extreme microgeographic adaptation: an integrated approach identifies a major gene underlying leaf trichome divergence in yellowstone *mimulus guttatus*. *Molecular Ecology* 25:5647–5662.
- Kawecki, T. J., and D. Ebert. 2004. Conceptual issues in local adaptation. *Ecology letters* 7:1225–1241.
- Keller, I., J. M. Alexander, R. Holderegger, and P. J. Edwards. 2013. Widespread phenotypic and genetic divergence along altitudinal gradients in animals. *Journal of evolutionary biology* 26:2527–2543.
- Kirkpatrick, M., and S. L. Nuismer. 2004. Sexual selection can constrain sympatric speciation. *Proc. Biol. Sci* pages 687–693.
- Kondrashov, A. S., and M. Shpak. 1998. On the origin of species by means of assortative mating. *Proceedings of the Royal Society of London. Series B: Biological Sciences* 265:2273–2278.
- Kopp, M., M. R. Servedio, T. C. Mendelson, R. J. Safran, R. L. Rodríguez, M. E. Hauber, E. C. Scordato, L. B. Symes, C. N. Balakrishnan, D. M. Zonana, and G. S. van Doorn. 2018. Mechanisms of Assortative Mating in Speciation with Gene Flow: Connecting Theory and Empirical Research. *The American Naturalist* 191:1–20.
- Lande, R. 1976. Natural selection and random genetic drift in phenotypic evolution. *Evolution* pages 314–334.
- . 1981. Models of speciation by sexual selection on polygenic traits. *Proceedings of the National Academy of Sciences* 78:3721–3725.

- Langin, K. M., T. S. Sillett, W. C. Funk, S. A. Morrison, M. A. Desrosiers, and C. K. Ghalambor. 2015. Islands within an island: Repeated adaptive divergence in a single population. *Evolution* 69:653–665.
- Langin, K. M., T. S. Sillett, S. A. Morrison, and C. K. Ghalambor. 2017. Bill morphology and neutral genetic structure both predict variation in acoustic signals within a bird population. *Behavioral Ecology* 28:866–873.
- Levene, H. 1953. Genetic equilibrium when more than one ecological niche is available. *The American Naturalist* 87:331–333.
- Maynard-Smith, J. 1966. Sympatric speciation. *The American Naturalist* 100:637–650.
- Metropolis, N., A. W. Rosenbluth, M. N. Rosenbluth, A. H. Teller, and E. Teller. 1953. Equation of state calculations by fast computing machines. *The journal of chemical physics* 21:1087–1092.
- Mikles, C. S., S. M. Aguillon, Y. L. Chan, P. Arcese, P. M. Benham, I. J. Lovette, and J. Walsh. 2020. Genomic differentiation and local adaptation on a microgeographic scale in a resident songbird. *Molecular Ecology* 29:4295–4307.
- Morrison, S. A., T. S. Sillett, C. K. Ghalambor, J. W. Fitzpatrick, D. M. Graber, V. J. Bakker, R. Bowman, C. T. Collins, P. W. Collins, K. S. Delaney, et al. 2011. Proactive conservation management of an island-endemic bird species in the face of global change. *BioScience* 61:1013–1021.
- Nature Conservancy. 2007. Santa Cruz Island Vegetation, 2005 The Nature Conservancy, San Diego, California, USA.
- Nicolaus, M., and P. Edelaar. 2018. Comparing the consequences of natural selection, adaptive phenotypic plasticity, and matching habitat choice for phenotype–environment matching, population genetic structure, and reproductive isolation in meta-populations. *Ecology and Evolution* 8:3815–3827.

- Peterson, A. T. 1993. Adaptive geographical variation in bill shape of scrub jays (*aphelocoma coerulescens*). *The American Naturalist* 142:508–527.
- Podos, J. 2001. Correlated evolution of morphology and vocal signal structure in darwin's finches. *Nature* 409:185–188.
- Pyle. 1997. Identification guide to North American birds, part i: Columbidae to Ploceidae. Slate Creek Press, Point Reyes, CA.
- R Core Team. 2021. R: A Language and Environment for Statistical Computing. R Foundation for Statistical Computing, Vienna, Austria. <http://www.r-project.org/>.
- Ravigné, V., U. Dieckmann, and I. Olivieri. 2009. Live Where You Thrive: Joint Evolution of Habitat Choice and Local Adaptation Facilitates Specialization and Promotes Diversity. *The American Naturalist* 174:E141–E169.
- Ravigné, V., I. Olivieri, and U. Dieckmann. 2004. Implications of habitat choice for protected polymorphisms .
- Richardson, J. L., M. C. Urban, D. I. Bolnick, and D. K. Skelly. 2014. Microgeographic adaptation and the spatial scale of evolution. *Trends in ecology & evolution* 29:165–176.
- Savolainen, O., M. Lascoux, and J. Merilä. 2013. Ecological genomics of local adaptation. *Nature Reviews Genetics* 14:807–820.
- Servedio, M. R., G. S. Van Doorn, M. Kopp, A. M. Frame, and P. Nosil. 2011. Magic traits in speciation:'magic'but not rare? *Trends in ecology & evolution* 26:389–397.
- Thibert-Plante, X., and A. P. Hendry. 2009. Five questions on ecological speciation addressed with individual-based simulations. *Journal of evolutionary biology* 22:109–123.
- Tigano, A., and V. L. Friesen. 2016. Genomics of local adaptation with gene flow. *Molecular ecology* 25:2144–2164.

Wolfram Research, Inc. 2021. Mathematica. Place: Champaign, Illinois.

Wright, S. 1946. Isolation by Distance under Diverse Systems of Mating. *Genetics* 31:39–59.

———. 1949. The genetical structure of populations. *Annals of eugenics* 15:323–354.

References Cited Only in the Online Enhancements

Brooks, S. P., and A. Gelman. 1998. General methods for monitoring convergence of iterative simulations. *Journal of computational and graphical statistics* 7:434–455.

Gelman, A., W. R. Gilks, and G. O. Roberts. 1997. Weak convergence and optimal scaling of random walk metropolis algorithms. *The annals of applied probability* 7:110–120.

Geweke, J. 1992. Evaluating the accuracy of sampling-based approaches to the calculations of posterior moments. *Bayesian statistics* 4:641–649.

Hadfield, J. D. 2010. Mcmc methods for multi-response generalized linear mixed models: The MCMCglmm R package. *Journal of Statistical Software* 33:1–22.

Makowski, D., M. S. Ben-Shachar, and D. Lüdecke. 2019. bayestestr: Describing effects and their uncertainty, existence and significance within the bayesian framework. *Journal of Open Source Software* 4:1541.

Plummer, M., N. Best, K. Cowles, and K. Vines. 2006. Coda: Convergence diagnosis and output analysis for mcmc. *R News* 6:7–11.

Figure Legends

Figure 1: Distributions of male and female bill length (mm) in the oak and pine habitats made from empirical measurements of individual captured island scrub-jays. Histograms show the raw data, solid curves represent kernel density estimates, and dashed vertical lines represent the mean of each distribution. Mean bill lengths and 95% confidence intervals for male oak birds was 24.78 ± 0.16 , female oak birds was 22.70 ± 0.16 , male pine birds was 25.57 ± 0.24 , and female pine birds was 23.50 ± 0.28 .

Figure 2: The life cycle and equations that specify the general model. N_i is the total number of individuals in subpopulation i , H_i is the proportional size of habitat i , z_m and z_f denote male and female trait values, respectively, α is the strength of mate preference, δ is the match offset value, z represents the trait values of either a male or female, m is the rate of random dispersal, η is the strength of habitat preference, θ_i and θ_j are the fixed ecological optima in each habitat, and γ is the strength of natural selection.

Figure 3: Probability an individual will disperse to a foreign habitat as a function of their trait value (z) relative to the fixed ecological optima in each habitat (θ_i and θ_j), random dispersal rate (m), the proportional size of each habitat (H_i and H_j), and the strength of habitat preference (η). Dashed vs. solid lines represent the probability of switching habitats depending on the point of origin. **A** The dispersal probabilities are symmetric when $H_i = H_j$. **B** The dispersal probabilities are asymmetric when $H_i \neq H_j$.

Figure 4: Bivariate posterior distributions give a depiction of the interactions between parameters by showing the densities of the parameter combinations for **A** Natural selection (γ) vs. Habitat preference (η), **B** Habitat preference (η) vs. Distance between the ecological optima (δ_θ), and **C** Distance between the ecological optima (δ_θ) vs. Natural Selection (γ). The marginal dis-

tributions of each parameter on the x-axis are displayed on the top of each bivariate plot.

Figure 5: Distributions of divergence in bill length (mm) between the oak and pine habitats in males and females that were generated by re-sampling the multivariate posterior distribution and re-simulating the IBS with the strength of mate preference (α) set equal to zero. Histograms show the simulated distributions and solid curves represent kernel density estimates. Black dashed vertical lines in each panel represent the mean of the null distributions of δ_z with no mate preference for males and females, and the black solid interval on the x-axis represents the 95% confidence interval for each null distribution. The blue vertical lines represent the empirical measure of male and female divergence (δ_z) in the island scrub-jay.

Figure 1

This is the author's accepted manuscript without copyediting, formatting, or final corrections. It will be published in an upcoming issue of *The American Naturalist*, published by The University of Chicago Press. Include the DOI when citing or quoting:
<https://doi.org/10.1086/72723>. Copyright 2023 The University of Chicago.

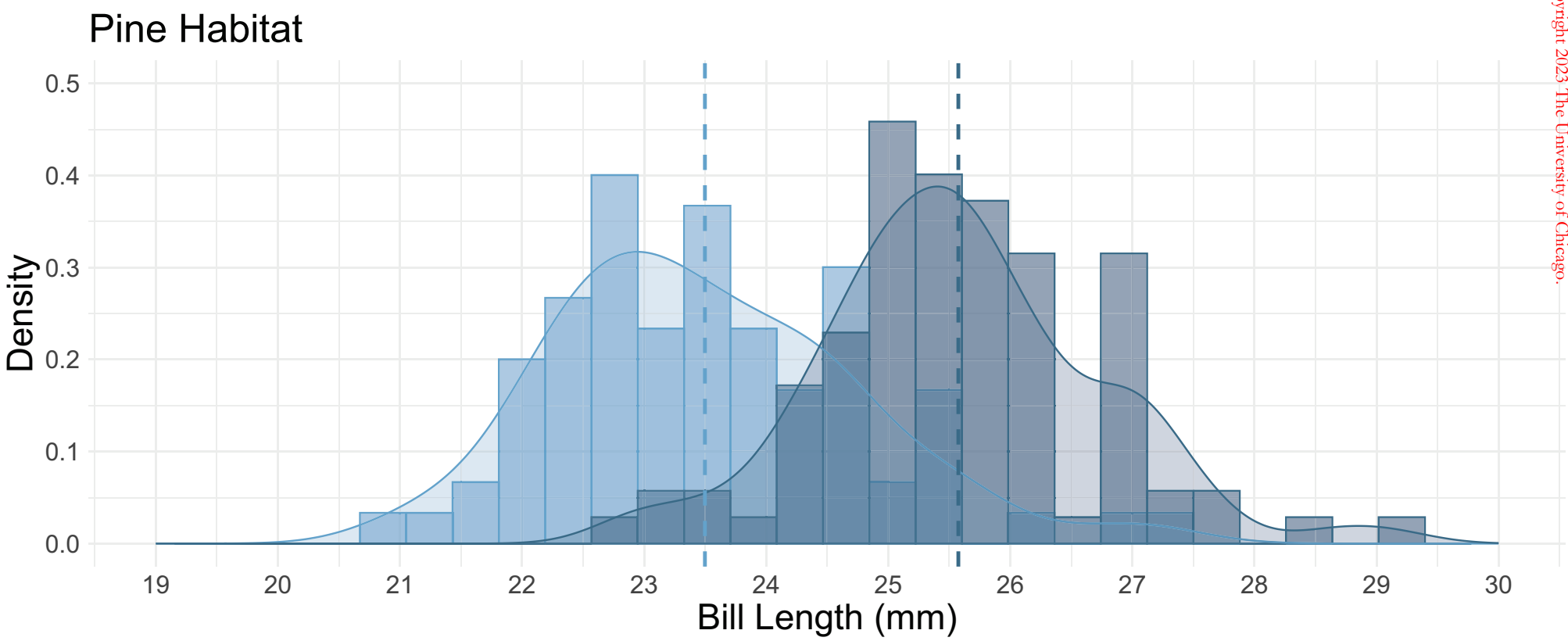
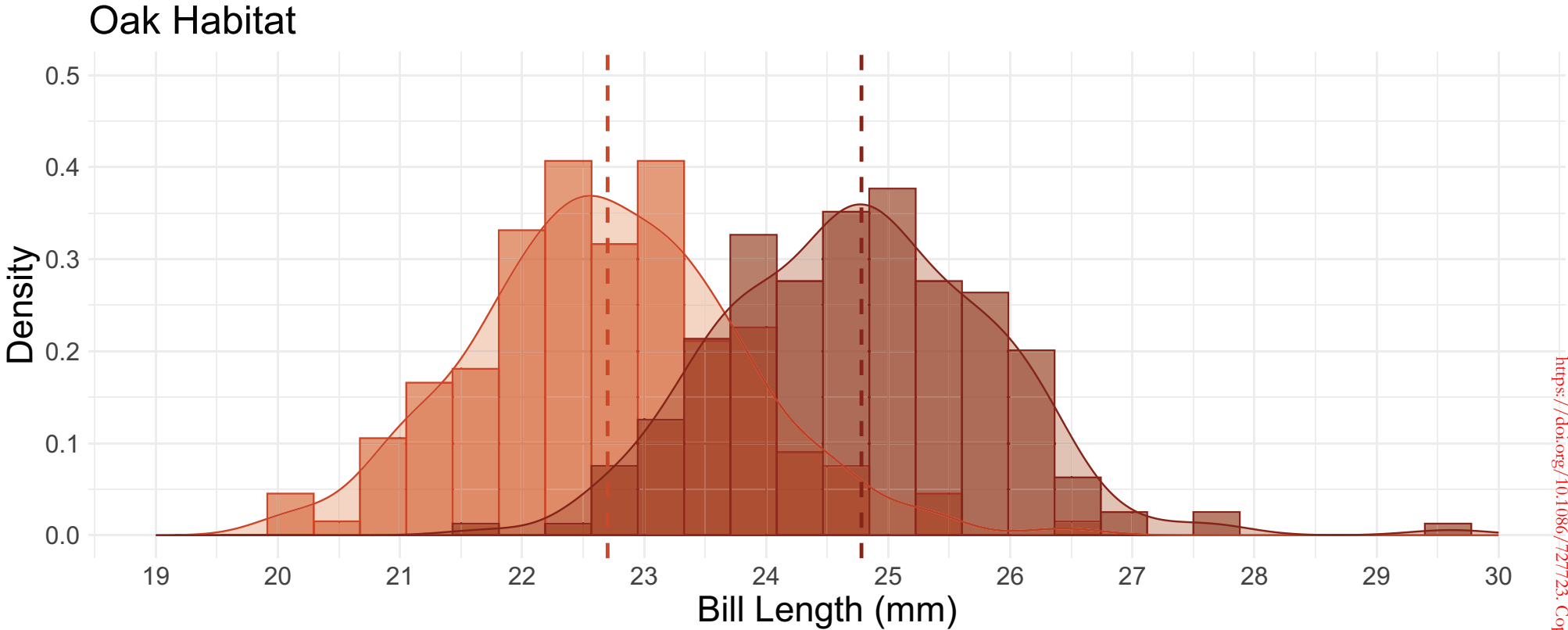


Figure 2

This is the author's accepted manuscript without copyediting, formatting, or final corrections. It will be published in its final form in an upcoming issue of *The American Naturalist*, published by The University of Chicago Press. Include the DOI when citing or quoting:
<https://doi.org/10.1086/72723>. Copyright 2023 The University of Chicago.

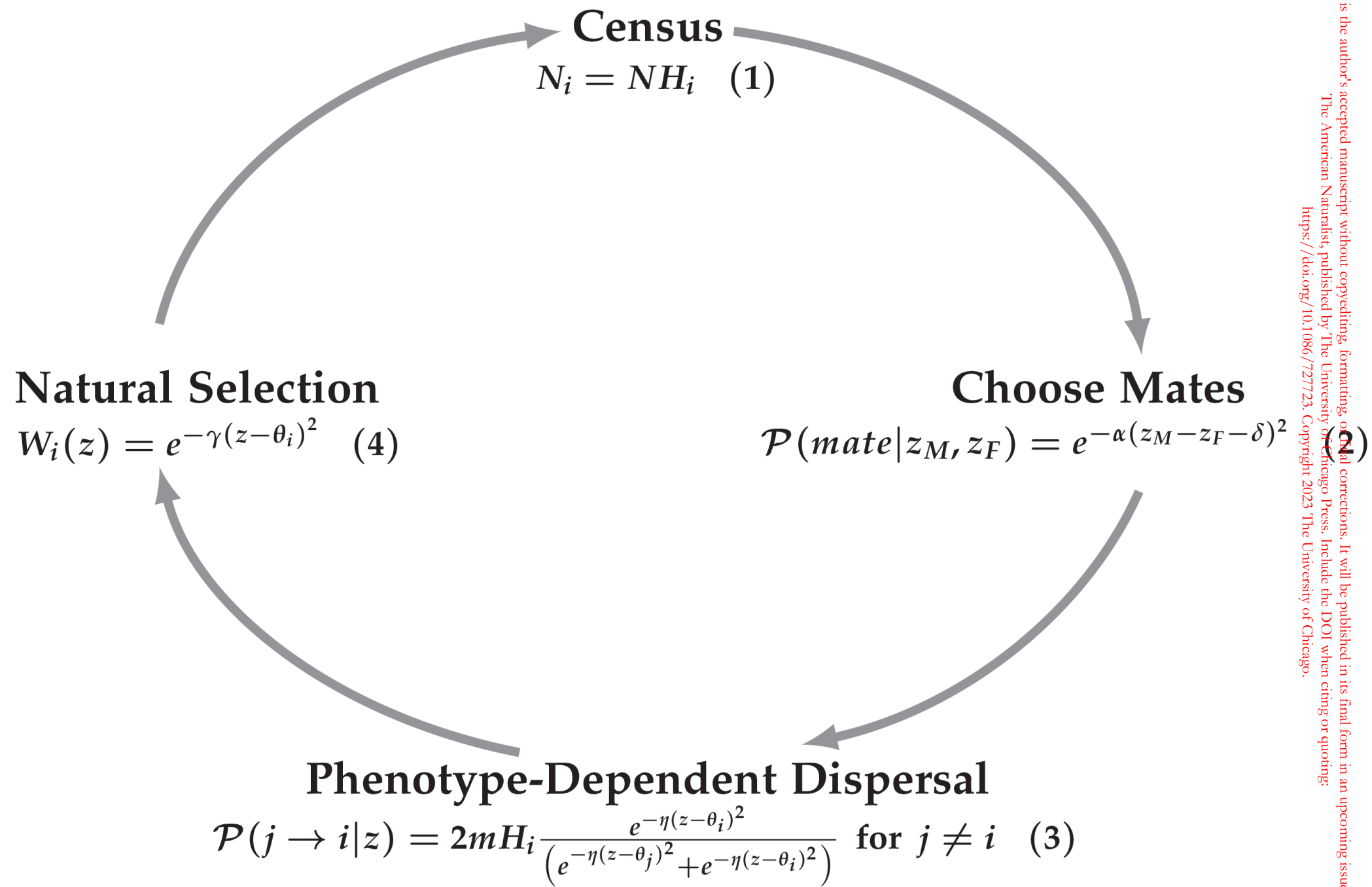
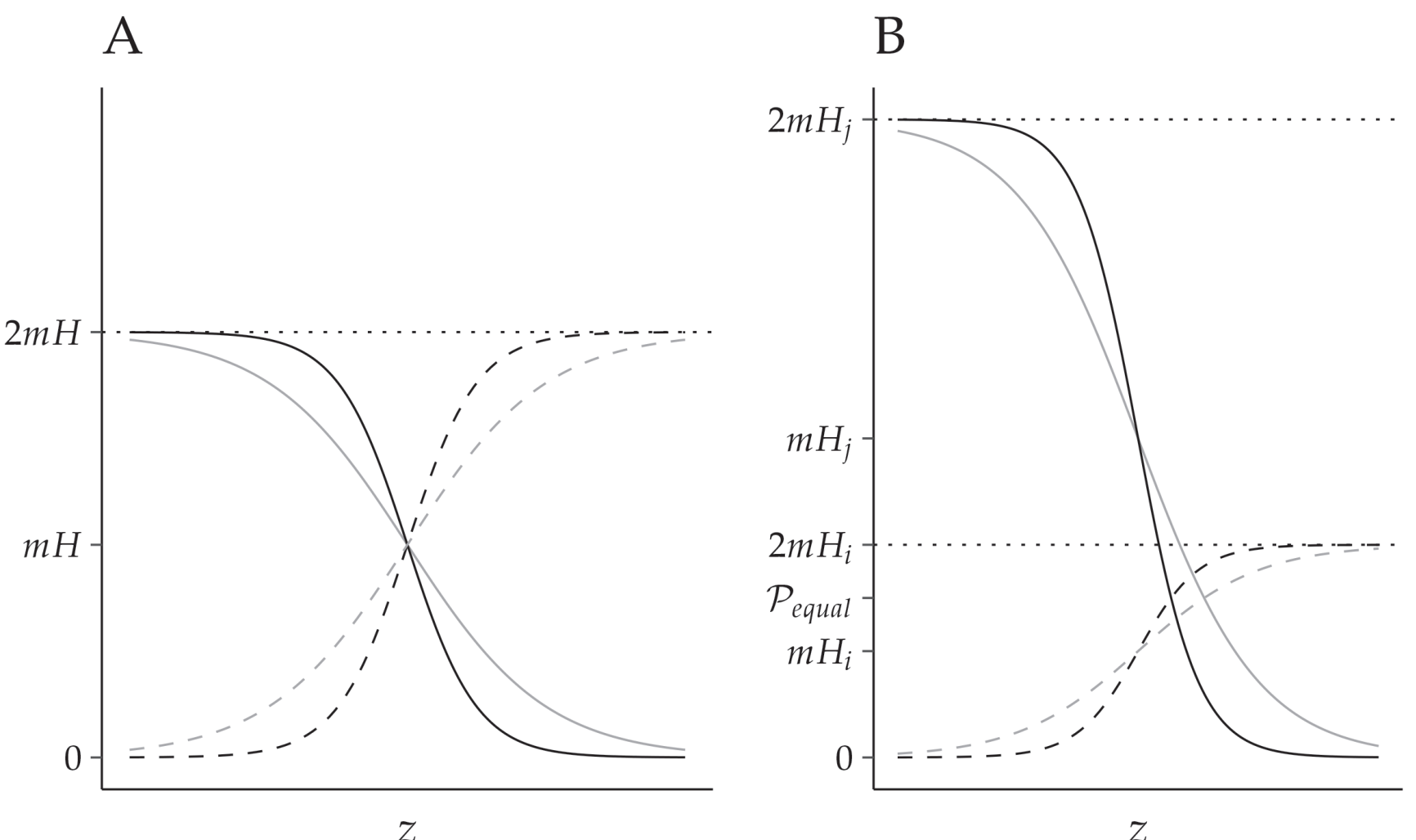


Figure 3 This is the author's accepted manuscript without copyediting, formatting, or final corrections. It will be published in its final form in an upcoming issue of The American Naturalist, published by The University of Chicago Press. Include the DOI when citing or quoting:
<https://doi.org/10.1086/727723>. Copyright 2023 The University of Chicago.

6.1
6.2



A

B

η

$2mH$

mH

0

N

$2mH_j$

mH_j

$2mH_i$

P_{equal}

mH_i

0

N

η

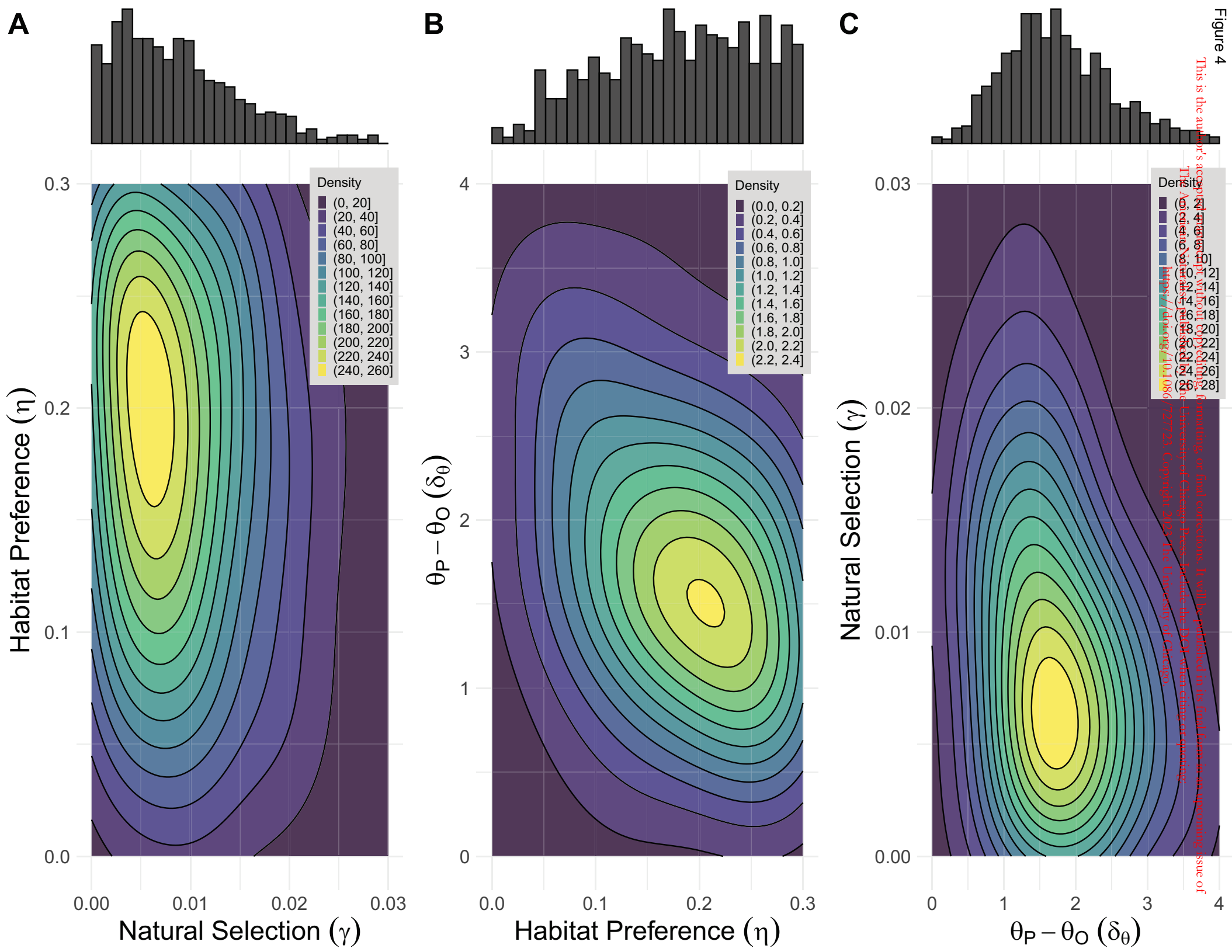
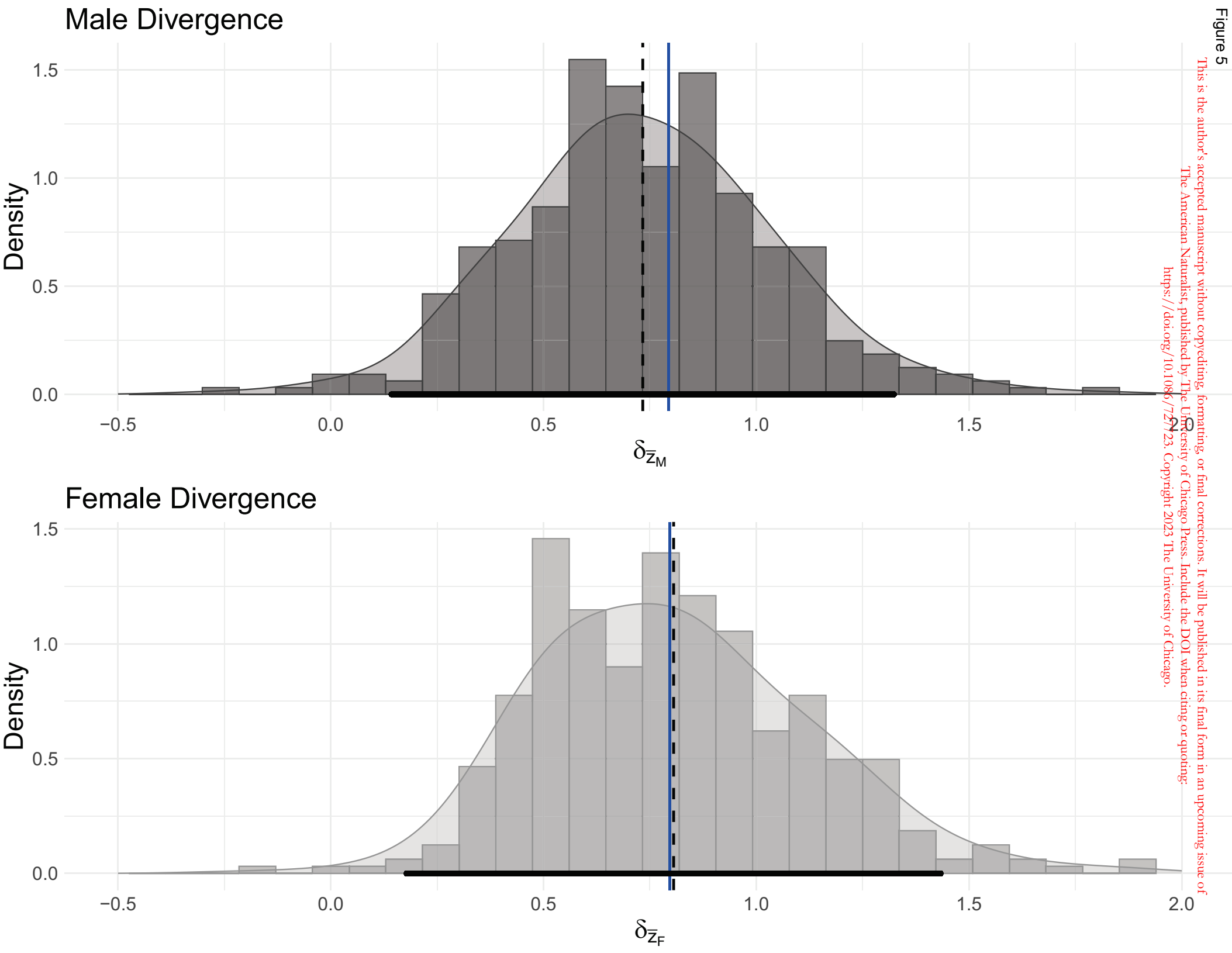


Figure 5

This is the author's accepted manuscript without copyediting, or final corrections. It will be published in its final form in an upcoming issue of *The American Naturalist*, published by The University of Chicago Press. Include the DOI when citing or quoting:
<https://doi.org/10.1086/72723>. Copyright 2023 The University of Chicago.



Online Supplement:

Unraveling Adaptive Divergence at Microgeographic Scales

The American Naturalist

Erin Clancey^{1,2,*}, Ailene MacPherson³, Rebecca G. Cheek⁴, James C. Mouton⁵,
T. Scott Sillett⁵, Cameron K. Ghalambor^{4,6}, W. Chris Funk⁴ & Paul A. Hohenlohe^{1,7}

1. Department of Mathematics and Statistical Science, University of Idaho, Moscow, ID 83844 USA;
2. Current Address: Paul G. Allen School for Global Health, Washington State University, Pullman, WA 99164 USA;
3. Department of Mathematics, Simon Fraser University, Burnaby, BC, V5A 1S6, Canada;
4. Graduate Degree Program in Ecology, Department of Biology, Colorado State University, Fort Collins, Colorado 80523 USA;
5. Migratory Bird Center, Smithsonian's National Zoo and Conservation Biology Institute, Washington, DC 20013;
6. Department of Biology, Centre for Biodiversity Dynamics (CBD), Norwegian University of Science and Technology (NTNU), N-7491 Trondheim, Norway;
7. Department of Biological Sciences, Institute for Bioinformatics and Evolutionary Studies, University of Idaho, Moscow, ID 83844 USA;

* Corresponding author; e-mail: erin.clancey@wsu.edu

Appendix A: Supplement to the Analytical Approximations

To obtain analytical approximations for the subpopulation phenotypic means in each habitat after reproduction (\bar{z}'_i) and dispersal (\bar{z}''_i), we can expand Equation (2) such that we have three integrals in the numerator and three integrals in the denominator (as shown in the supporting Mathematica Notebook):

$$\bar{z}''_i = \frac{\int_{-\infty}^{\infty} z f'_i(z) N H_i dz - \int_{-\infty}^{\infty} z f'_i(z) N H_i \mathcal{P}(i \rightarrow j|z) dz + \int_{-\infty}^{\infty} z f'_j(z) N H_j \mathcal{P}(j \rightarrow i|z) dz}{\int_{-\infty}^{\infty} f'_i(z) N H_i dz - \int_{-\infty}^{\infty} f'_i(z) N H_i \mathcal{P}(i \rightarrow j|z) dz + \int_{-\infty}^{\infty} f'_j(z) N H_j \mathcal{P}(j \rightarrow i|z) dz}. \quad (\text{A1})$$

We can simplify the expression in Equation (A1) slightly to show the integrals that remain and require approximation:

$$\bar{z}''_i = \frac{\bar{z}'_i H_i - H_i \int_{-\infty}^{\infty} z f'_i(z) \mathcal{P}(i \rightarrow j|z) dz + H_j \int_{-\infty}^{\infty} z f'_j(z) \mathcal{P}(j \rightarrow i|z) dz}{H_i - H_i \int_{-\infty}^{\infty} f'_i(z) \mathcal{P}(i \rightarrow j|z) dz + H_j \int_{-\infty}^{\infty} f'_j(z) \mathcal{P}(j \rightarrow i|z) dz}. \quad (\text{A2})$$

Here, $f_i(z)'$ is the phenotypic trait distribution in habitat i after mating and reproduction which is assumed to be a normal distribution, and $\mathcal{P}(i \rightarrow j|z)$ is given in Figure 1 Equation (3) in the general model. We assume θ_j is larger than θ_i , and define the mean of the optima as $\mu_\theta = \frac{1}{2}(\theta_i + \theta_j)$. We also define $\delta_\theta = \theta_j - \theta_i$, $\delta_{z,\mu_\theta} = z - \mu_\theta$, and $\delta_{\bar{z}_i,\mu_\theta} = \bar{z}_i - \mu_\theta$. Importantly, we make the five assumptions described in the main text in the Analytical Approximations section. We explicitly assume $z - \theta_i$ is small and of $\mathcal{O}(\epsilon)$, and δ_θ is small and of $\mathcal{O}(\epsilon)$. A result of these assumptions is that the distance between the subpopulation means is also small and of $\mathcal{O}(\epsilon)$, and the phenotypic variance (\mathcal{V}_z) is also small and of order $\mathcal{O}(\epsilon^2)$. Thus, we can write $\delta_\theta = \tilde{\delta}_\theta \epsilon$, $\delta_{z,\mu_\theta} = \tilde{\delta}_{z,\mu_\theta} \epsilon$, $\delta_{\bar{z}_i,\mu_\theta} = \tilde{\delta}_{\bar{z}_i,\mu_\theta} \epsilon$, and $\mathcal{V}_z = \tilde{\mathcal{V}}_z \epsilon^2$. With these assumptions, we make the following replacements:

$$\theta_i = \mu_\theta - \frac{1}{2} \tilde{\delta}_\theta \epsilon,$$

$$\theta_j = \mu_\theta + \frac{1}{2} \tilde{\delta}_\theta \epsilon,$$

$$z = \mu_\theta + \tilde{\delta}_{z,\mu_\theta} \epsilon,$$

$$\bar{z}_i = \mu_\theta + \tilde{\delta}_{\bar{z}_i,\mu_\theta} \epsilon,$$

$$\bar{z}_j = \mu_\theta + \tilde{\delta}_{\bar{z}_j,\mu_\theta} \epsilon,$$

and Taylor Series expand each integral in the numerator and denominator of Equation (A1) to $\mathcal{O}(\epsilon^2)$. This gives us approximations for the subpopulation means after dispersal:

$$\bar{z}_i'' \approx \bar{z}_i(1 - mH_j) + \bar{z}_j mH_j \quad (\text{A3a})$$

$$\bar{z}_j'' \approx \bar{z}_j(1 - mH_i) + \bar{z}_i mH_i. \quad (\text{A3b})$$

Notice here that when we make our assumptions and approximate to $\mathcal{O}(\epsilon^2)$, habitat preference (η) no longer has a diversifying effect on the subpopulation means.

To find the subpopulation means after dispersal and selection (\bar{z}_i''') we make the same replacements as in Equation (A1) and apply a second order, $\mathcal{O}(\epsilon^2)$, Taylor Series expansion to Equation (3), originally formulated by Lande (1976), giving us

$$\Delta \bar{z}_i''' = G \frac{d}{d\bar{z}_i''} \mathbb{E} \left[e^{-\gamma(z-\theta_i)^2} \right] \approx \frac{2G\gamma(\theta_i - \bar{z}_i'')}{1 - \gamma(\mathcal{V}_z - (\bar{z}_i'' - \theta_i)^2)}, \quad (\text{A4})$$

the change in mean phenotype after selection in one generation. The trait means in each subpopulation after reproduction, dispersal, and selection are thus

$$\bar{z}_i''' \approx \bar{z}_i''(mH_j - 1)(2G\gamma - 1) + \bar{z}_j''mH_j(1 - 2G\gamma) + 2G\gamma\theta_i \quad (\text{A5a})$$

$$\bar{z}_j''' \approx \bar{z}_j''(mH_i - 1)(2G\gamma - 1) + \bar{z}_i''mH_i(1 - 2G\gamma) + 2G\gamma\theta_j. \quad (\text{A5b})$$

Solving the set of recursions in Equations (A4a) and (A4b) gives us the trait means of each subpopulation at evolutionary equilibrium:

$$\bar{z}_{eq_i} \approx \frac{m(2G\gamma - 1)(H_i\theta_i + H_j\theta_j) - 2G\gamma\theta_j}{2G\gamma(m - 1) - 1} \quad (\text{A6a})$$

$$\bar{z}_{eq_j} \approx \frac{m(2G\gamma - 1)(H_i\theta_i + H_j\theta_j) - 2G\gamma\theta_i}{2G\gamma(m - 1) - m}. \quad (\text{A6b})$$

Now we can find the difference $\delta_{\bar{z}_{eq}} = \bar{z}_{eq_j} - \bar{z}_{eq_i}$ to obtain a solution for phenotypic divergence at equilibrium which gives us Equation (4) in the main text.

Appendix B: Supplement to the Individual-Based Simulations and Bayesian Parameter Estimation

As described in the main text, we used individual-based simulations (IBS) to relax key assumptions of the analytical model and apply our model to the island scrub-jay. Evaluation of our IBS relied on the population reaching evolutionary equilibrium. Figure B1 shows an example of the male and female subpopulation means and variances at equilibrium after 1,000 generations when the parameters are set equal to the estimated parameter values show in Table 2 in the main text.

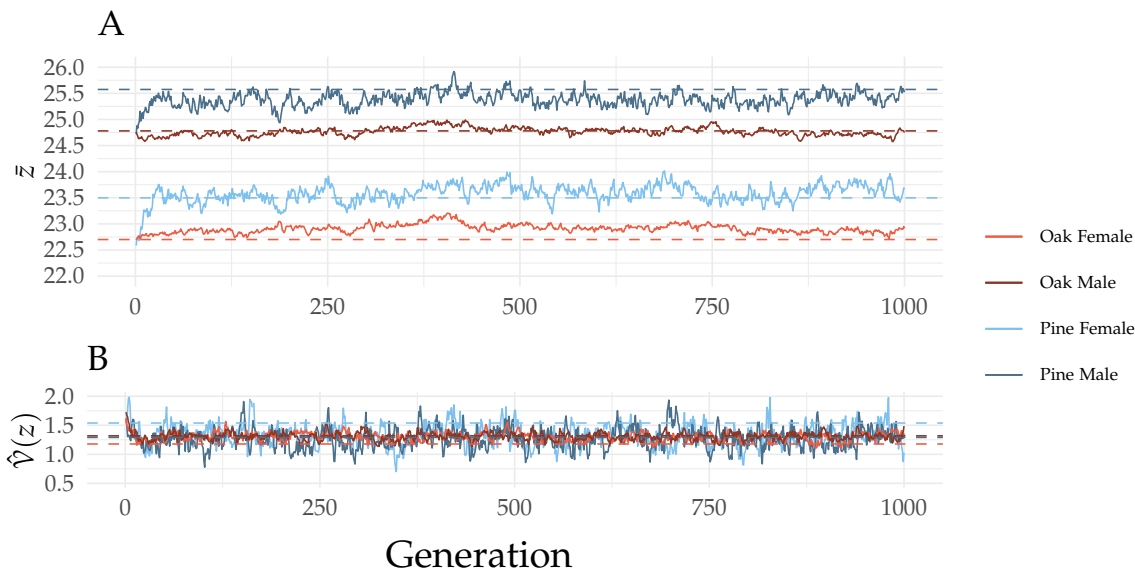


Figure B1: Results of one simulation run over 1,000 generations. **A** Male and female pine and oak subpopulation mean phenotypes (\bar{z}). Solid lines represent the means for every generation of the simulation and dashed lines represent the empirical sample means. **B** Population variances for male and female pine and oak subpopulations. Solid lines represent the variances for every generation of the simulation, and dashed lines represent empirical sample variances.

We used our individual-based simulations (IBS) to estimate the parameters in our model with the data on bill length (mm) in the island scrub-jay. We implemented the Metropolis-Hastings algorithm to sample from the joint posterior distribution of our IBS model parameters and estimate the unknown values. To implement the Metropolis-Hastings algorithm (Metropolis

et al., 1953), we used an adaptive approach to choose the proposal distribution and we simulated the life cycle using our IBS to evaluate the value of the likelihood function given in Equation (5) in the main text during each iteration. To find an appropriate proposal distribution, we began with a pilot run of one chain with 1,000 iterations drawing starting parameter values at random with a multivariate proposal distribution with zero covariance, and the covariance matrix scalar, c , set equal to 1. The scalar, c , is a function of the acceptance probability, p , of the samples in the Metropolis-Hastings algorithm and the CDF of the standard normal density, ϕ (Gelman et al., 1997), such that the updated value of c can be calculated as $c_{new} = \frac{c_{current}\Phi^{-1}(p_{optimal}/2)}{\Phi^{-1}(p_{current}/2)}$. The optimal acceptance probability, $p_{optimal}$, for the Markov chain asymptotically approaches 0.234-0.238 for higher dimensional problems (Gelman et al., 1997). After our first pilot run, we iteratively updated the proposal covariance matrix, the matrix scalar, and the parameter starting values over five more consecutive 1,000 pilot runs, where the covariance matrix was estimated from the posterior distribution of each pilot run, the scalar was calculated using the formula above given the current acceptance probability, and the new starting values were the means of the former pilot chain. Once we obtained our final proposal distribution, we ran five chains for 30,000 iterations using the resources of the Center for Institutional Research Computing at Washington State University.

To assess each chain we used the Geweke diagnostic (Geweke, 1992) to determine convergence within each chain, and the Gelman diagnostic (Brooks and Gelman, 1998) to determine convergence among chains. We used the Geweke diagnostic to compare the mean of the first quarter of each chain to the mean of the last half of each chain. All chains converged except for θ_P and ϵ_e in Chain 2, which had Z-scores of -2.49 and -2.51 respectively. The Gelman diagnostic compares the variance within each chain to variance among all the chains. The ratios of the variance within and among the chains all had upper bounds ≤ 1.06 for all parameters demonstrating that we reached global convergence. Serial correlation was high in our samples, and therefore we discarded the first 200 samples for burn-in and thinned each chain by keeping every 200th sample to obtain a sample of 750 points in the posterior distribution. All pairwise correlations between

parameters values were calculated from the processed joint posterior distribution. Processing of the posterior distributions was performed using the package coda in R (Plummer et al., 2006).

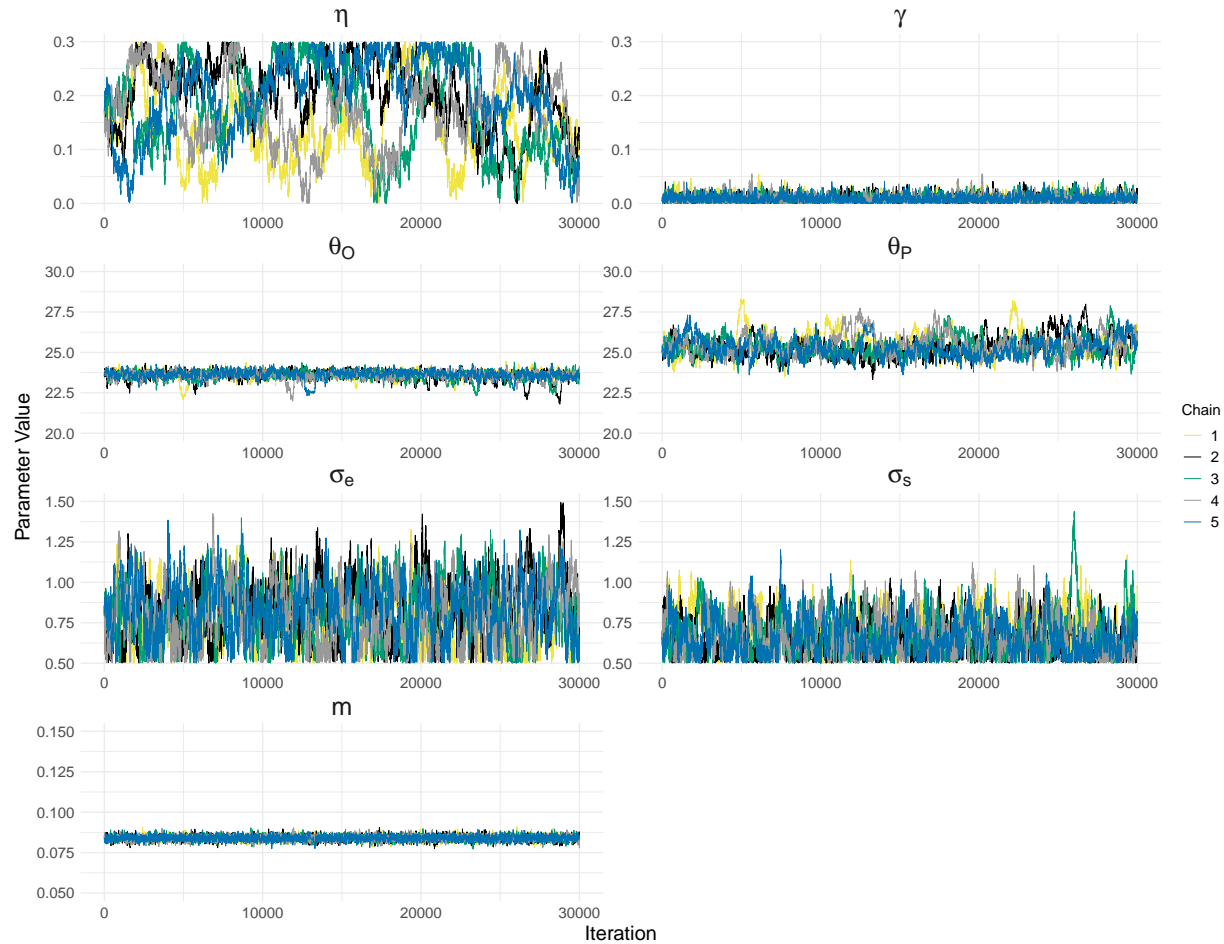


Figure B2: Trace plot of the five chains over 30,000 iterations for each parameter estimated in the model. The ranges on the y-axis of each plot reflect the ranges given by the prior distributions for each parameter.

To obtain point and interval estimates for each unknown parameter in the IBS, we estimated the mode and 95% Highest Density Interval (HDI) for each posterior distribution in Figure B3. We estimated the marginal parameter modes using kernel density estimation with a bandwidth of 2 using the package MCMCglmm: MCMC Generalised Linear Mixed Models in R (Hadfield, 2010). We obtained the 95% HDIs in R using bayestestR (Makowski et al., 2019). Numeric values of these estimates are given in Table 2 in the main text.

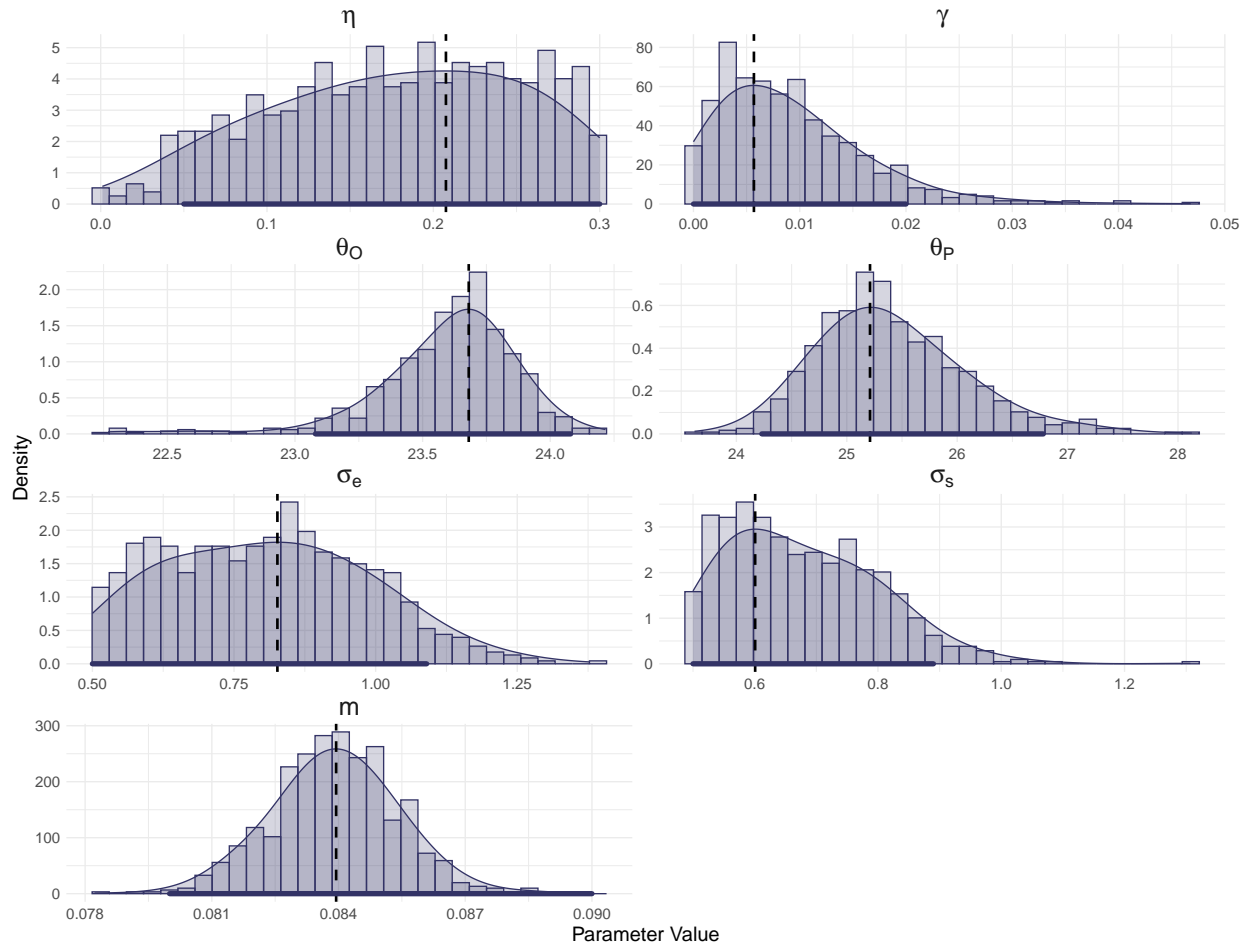


Figure B3: Marginal posterior density for each parameter estimated in the model. The black dashed line represents the posterior mode and the dark purple ribbon on the x-axis represents the 95% Highest Density Interval (HDI) for each parameter.

Literature Cited

- Brooks, S. P., and A. Gelman. 1998. General methods for monitoring convergence of iterative simulations. *Journal of computational and graphical statistics* 7:434–455.
- Gelman, A., W. R. Gilks, and G. O. Roberts. 1997. Weak convergence and optimal scaling of random walk metropolis algorithms. *The annals of applied probability* 7:110–120.
- Geweke, J. 1992. Evaluating the accuracy of sampling-based approaches to the calculations of posterior moments. *Bayesian statistics* 4:641–649.
- Hadfield, J. D. 2010. Mcmc methods for multi-response generalized linear mixed models: The MCMCglmm R package. *Journal of Statistical Software* 33:1–22.
- Lande, R. 1976. Natural selection and random genetic drift in phenotypic evolution. *Evolution* pages 314–334.
- Makowski, D., M. S. Ben-Shachar, and D. Lüdecke. 2019. bayestestr: Describing effects and their uncertainty, existence and significance within the bayesian framework. *Journal of Open Source Software* 4:1541.
- Metropolis, N., A. W. Rosenbluth, M. N. Rosenbluth, A. H. Teller, and E. Teller. 1953. Equation of state calculations by fast computing machines. *The journal of chemical physics* 21:1087–1092.
- Plummer, M., N. Best, K. Cowles, and K. Vines. 2006. Coda: Convergence diagnosis and output analysis for mcmc. *R News* 6:7–11.